



## A new group of late Oligocene mysticetes from México

Atzcalli Ehécatl Hernández Cisneros

### ABSTRACT

The Oligocene cetacean fossil record from Mexico represents an important element to understand the cetacean evolutionary history in the Pacific Basin. However, our knowledge of these fossils is poor, as the specimens have not yet been properly described. Nonetheless, recent observations on Oligocene fossils from the state of Baja California Sur offer new ideas with regard to the cetacean taxonomic composition and suggest a high diversity of mysticete fossils with several forms of toothless mysticetes. Consequently, a new group of extinct mysticetes from the late Oligocene (Chat-tian) of Mexico is described based on two different specimens (partial skulls), which share a phenetically similar periotic bone. These fossils were collected from the marine units of the San Juan Member (30 to 23 Ma) of the El Cien Formation in Baja California Sur. Furthermore, this new group of archaic mysticetes is distinct to eomysticetid-like animals, *Mauicetus*, *Horopeta*, and *Whakakai* mainly in the periotic morphology specifically in: a longer and anteroposteriorly flattened compound posterior process of the periotic, and a periotic (pars cochlearis, anterior process and body of the periotic) with an ovoid shape in lateral and medial views. Phylogenetic analysis suggests a closer relation to *Sitsqwayk* and eomysticetes than to *Horopeta+Whakakai* and crown Mysticeti. Oligocene cetaceans from Mexico are still poorly known in terms of their paleoecology and phyletic relationship. This work represents the first description of Oligocene mysticetes from Baja California Sur and shows the potential to further understanding of the biogeographic history of mysticetes in the Eastern Pacific.

Atzcalli Ehécatl Hernández Cisneros. Instituto Politécnico Nacional–Centro Interdisciplinario de Ciencias Marinas. Address: Av. Instituto Politécnico Nacional, Playa Palo de Santa Rita. Postal mail 592, 23096, La Paz, Baja California Sur, Mexico, and Museo de Historia Natural de la Universidad Autónoma de Baja California Sur, Universidad Autónoma de Baja California Sur. Address: Carretera al Sur Km 5.5, Postal mail 19-B, 23080, La Paz, Baja California Sur, México. atz\_nemesis@hotmail.com

Keywords: Cetacea; Mysticeti; new species; Oligocene; El Cien Formation; Baja California Sur

Submission: 16 November 2016 Acceptance: 26 February 2018

---

<http://zoobank.org/138AE090-E19F-442E-8BDF-13B8401B755E>

Hernández Cisneros, Atzcalli Ehécatl. 2018. A new group of late Oligocene mysticetes from México. *Palaeontologia Electronica* 21.1.7A 1-30. <https://doi.org/10.26879/746>  
[palaeo-electronica.org/content/2018/2147-oligocene-mysticetes-from-mexico](http://palaeo-electronica.org/content/2018/2147-oligocene-mysticetes-from-mexico)

Copyright: March 2018 Instituto Politécnico Nacional – Centro Interdisciplinario de Ciencias Marinas.

This is an open access article distributed under the terms of the Creative Commons Attribution License, which permits unrestricted use, distribution, and reproduction in any medium, provided the original author and source are credited.  
[creativecommons.org/licenses/by/4.0/](http://creativecommons.org/licenses/by/4.0/)

## INTRODUCTION

The Oligocene cetacean radiation is known as an important step in the evolution and establishment of stem Mysticeti and Odontoceti, and the development of filter-feeding and echolocation as singular adaptations of each group, respectively (Fordyce, 2009a, 2009b). However, knowledge of taxonomic diversity of Oligocene cetaceans is limited mainly due to undiscovered fossils, or unpublished data (Uhen and Pyenson, 2007). Hence, in groups such as Mysticeti an important informative gap exists regarding its estimated early diversity during the Oligocene. This epoch is interpreted as an inflexion point rich in taxonomical diversity, evolutionary traits, and is a key to untangling relations between stem and crown mysticetes (Whitmore and Sanders, 1976; Fordyce, 1980, 1992, 2003). Nevertheless, the Oligocene Mysticeti taxonomic composition in the Pacific Ocean has increased recently by descriptions of new species (e.g., Peredo and Uhen, 2016, Geisler et al., 2017). Currently there are about 28 recognized species of Oligocene mysticetes, mainly aetiocetids and eomysticetes (Hernández-Cisneros et al., 2017), in a range of ~33 to 24 Ma (see Marx and Fordyce, 2015), which represent a portion of the known materials and sites (Fordyce, 2009c, 2009d).

Indeed, a place like Mexico offers an important Oligocene cetacean fossil record that is poorly known (Barnes, 1998), but recent advances (Hernández-Cisneros, et al., 2017) suggest a more complete idea on its diversity. The main Oligocene fossiliferous area with cetaceans in Mexico is located in the state of Baja California Sur, which is recognized as the most important southern record of North America, and its fossils include tooth-bearing mysticetes (aetiocetids) and toothless mysticetes, as well as archaic odontocetes, and possible *Kekenodon*-like animals from the late Oligocene of El Cien Formation and San Gregorio Formation (Hernández-Cisneros and Tsai, 2016; Hernández-Cisneros et al., 2017).

In this paper, a new taxon of mysticetes is described based on two specimens housed in the paleontological collection of the Museo de Historia Natural de la Universidad Autónoma de Baja California Sur. These fossils were collected from the San Juan Member, El Cien Formation, Baja California Sur, Mexico, with an estimated age of ~27 Ma, representing the first Oligocene mysticetes described from Mexico. Both are added to the short list of Oligocene mysticetes classified as non-eomysticetes animals which include: *Mauicetus parki* Benham, 1937, *Horopeta umarere* Tsai and

Fordyce, 2015a, *Whakakai waipata* Tsai and Fordyce, 2016, and *Sitsqwayk cornishorum* Peredo and Uhen, 2016. In addition, these Mexican fossils offer anatomical, ecological, and biogeographic details to the poorly known Oligocene Chaeomysticeti in the Pacific Ocean.

## MATERIAL AND METHODS

Descriptions are based on two different partial skulls: MHN-UABCS\_EcSj5/06/31 and MHN-UABCS\_EcSj5/18/95. From here on MHN-UABCS will be referred to as MU (see the complete specimen code in the material reference section below). Although fossil materials are fragmentary, there is enough morphological data to allow a reasonable phylogenetic and taxonomic analysis. Anatomical terms were based on Mead and Fordyce (2009), and measurements follow Boessenecker and Fordyce (2014) and Tsai and Fordyce (2015a). The standard ear bone views follow Mead and Fordyce (2009, p. 4) criteria for further comparison to the Cetacea, e.g., dorsal view is the surface of dorsal margin of the internal acoustic meatus. In addition, the phrase “head of the periotic” is a new anatomical term used to easily refer to the combination of the next anatomic elements: pars cochlearis, body of the periotic and anterior process, and can be considered as a compound anatomic term, which corresponds to the anterior portion of the periotic bone, excluding the posterior process and associated characters. Measurements are listed in Tables 1-3. Fossils were prepared using pneumatic chisels and hand tools; bones were glued and stabilized with polyvinyl acetate. Photos were taken with a Canon PowerShot G10 camera, and edited with Photoshop© and CorelDraw© software.

Cladistics analysis was performed using Marx and Fordyce (2015) data, plus modifications from Marx et al. (2015). Morphological characters and matrix were taken from www.morphobank.org (project 687). New states of character were added in character 120, new state (5), which is a straight and non-prominent outline of the postglenoid process in anterior or posterior views, character 146, new state (3), anterior process of the periotic in lateral view ovoid or anteroposteriorly compressed with an anterodorsal angle prominent as linguiform. The latter two states were added to reflect the autapomorphic features of the specimens. This analysis includes *Horopeta umarere* and *Whakakai waipata* from Tsai and Fordyce (2016) and *Sitsqwayk cornishorum* (Peredo and Uhen, 2016).

Phylogenetic results were obtained through T.N.T. software (Goloboff et al., 2008a) under heu-

**TABLE 1.** Skull measures in mm. No data (-), maximum preserved (\*), approximate measure (~).

	<i>Tlaxcallicetus</i> sp.	<i>Tlaxcallicetus guaycurae</i>
<b>Cranium</b>		
Anteroposterior length	*200	*270
Greatest anteroposterior length the exoccipital	-	91.6
Anteroposterior length of the zygomatic process of the squamosal	-	*150
Byzigomatic width	-	~750
Greatest transverse width of the supraoccipital	-	~370
Transverse width of exoccipitals	-	~248
Greatest Transverse width of occipital condyles	~125	126
Height of foramen magnum	45	40.2
Transverse width of foramen magnum	~47	~35.2
Width of upper intercondyloid notch	~49.72	43.1
Width of low intercondyloid notch	~26.1	21
Transverse width of basioccipital crest, at its middle length	26.68	34.9
Transverse width across basioccipital crest	~64.2	~90.3
Diameter of glenoid fossa (anterolateral-posteromedial axis)	-	139.5
Diameter of glenoid fossa (posterolateral-anteromedial axis)	-	118.6

ristic parsimony analysis using the 'traditional search' option. Characters were treated under equal weights and implied weights. A backbone constraint tree (see Swofford, 1991) was applied as in Geisler et al. (2011), following the molecular tree from Gatesy et al. (2013, figure 6). Although the implied weights method (Goloboff, 1993; Goloboff et al., 2008b) was considered problematic due to its potential to produce false tree topologies (see Congreve and Lamsdell, 2016), it was not discarded taking into account consistency in cetacean phylogeny between parsimony analysis and probabilistic methods as Bayesian inference of past studies (e.g., Geisler et al., 2011; Marx and Fordyce, 2015; Marx et al., 2015). Three different concavity constants ( $k = 3, 6$  and  $9$ ) were used to test phylogenetic results of implied weights analysis. The latter was made taking into account the warning about not using it conclusively to determine sister taxon relations, and under the criterion of not discarding previous topologies from implied weights analysis (Congreve and Lamsdell, 2016). Only the consensus tree under  $k=6$  value is illustrated due to the fact that it is the lowest value of  $k$ , which fits with the general tree topology from Marx et al. (2015). Settings include a 10,000-random stepwise-addition replicate (in Memory option), and tree bisection reconnection (TBR) branch swapping with 10 trees per replicate. An additive option was applied as an equivalent to the ordered setting to 25 ordered characters of Marx and Fordyce (2015). Multiple most parsimonious trees were

summarized using strict consensus. Support values were obtained by symmetric resampling based on 2000 replicates and reported as GC frequency differences (Goloboff et al. 2003). Character code, and character state maps, as well as cladistic data, are available in Appendices 1-6. Preliminary tree images and characters map were obtained using Winclada software (Nixon, 2002).

#### **Institutional Abbreviations**

**MHN-UABCS (MU)**, Museo de Historia Natural de la Universidad Autónoma de Baja California Sur, La Paz, Baja California Sur, Mexico.

#### **GEOLOGICAL SETTING**

Fossils MU EcSj5/06/31 and MU EcSj5/18/95 were collected from the El Saladito locality (24.43916 N, -110.69512 W), San Juan de la Costa, in the west coast of Bahía de La Paz 50 km north of La Paz, Baja California Sur, Mexico (Figure 1). Late Oligocene outcrops at San Juan de la Costa belong to the San Juan Member, which is one of two geological subunits of the Oligocene age from El Cien Formation (Fischer et al., 1995; Plata-Hernández, 2002). The San Juan Member is mainly composed of laminated, partly tuffaceous, siliceous, diatomaceous or phosphatic mudstones, partly phosphatic silt- and sandstones, granular phosphorite, tuff and conglomerates (Fischer et al., 1995). San Juan Member's marine units reflect shelf, coast, lagoon, and delta depositional environments (Schwennicke, 1994), and several stud-

**TABLE 2.** Measurements in mm of ear bones. No data (-), maximum preserved (\*), approximate measure (~), not clear (?).

	<i>Tlaxcallicetus</i> sp.	<i>Tlaxcallicetus guaycurae</i>
<b>Left bulla</b>		
Anteroposterior length	*54.3	-
Greatest transverse width	44.7	-
Dorsoventral depth of involucrum, at anterior level to inner posterior pedicle	27.8	-
Transversal thickness of involucrum across the anterior point of the base of the inner posterior pedicle	28	-
Anteroposterior length of the tympanic cavity	*42.4	-
Greatest transverse width of inner posterior prominence/medial lobe	~22.9	-
Greatest transverse width of outer posterior prominence/lateral lobe	~20	-
<b>Left periotic</b>		
Greatest anteroposterior length	*54	~76.42
Anteroposterior length of the suprameatal area	7.2	-
Greatest anteroposterior length of anterior process, from anterior incisures to anterior keel	22.78	~20.7
Greatest length of the posterior process	-	~60.8
Maximum anteroposterior length of pars cochlearis	*28.74	~29.36
Greatest length of internal acoustic meatus	16.2	-
Greatest length of aperture for the cochlear aqueduct	~3.5	~2.5
Greatest length of aperture for the vestibular aqueduct	7.68	-
Greatest length of proximal opening of the facial canal	~4	-
Greatest length of dorsal vestibular area	8.2	-
Greatest length of fenestra rotunda	-	~2.4
Greatest length of fenestra ovalis	-	-
Greatest length of malleolar fossa	-	?
Greatest length of distal opening of the facial canal	-	6.4
Greatest length of stapedia muscle fossa	-	?
Transverse width of base of anterior process	-	10.5
Transverse width of pars cochlearis	17	?
Transverse width of the posterior process (anteroposterior plan)	-	17
Maximum transverse width of suprameatal area	10	-
Maximum transverse width of periotic, from the medial face of pars cochlearis to lateral wall of the periotic body	~30.9	?
Dorsoventral depth of anterior process	*55	*41.3

**TABLE 3.** Measurements in mm of left thyrohyoid bone. No data (-).

	<i>Tlaxcallicetus</i> sp.	<i>Tlaxcallicetus guaycurae</i>
Length	73	-
Width at middle	26.4	-
Thickness at middle	22.7	-

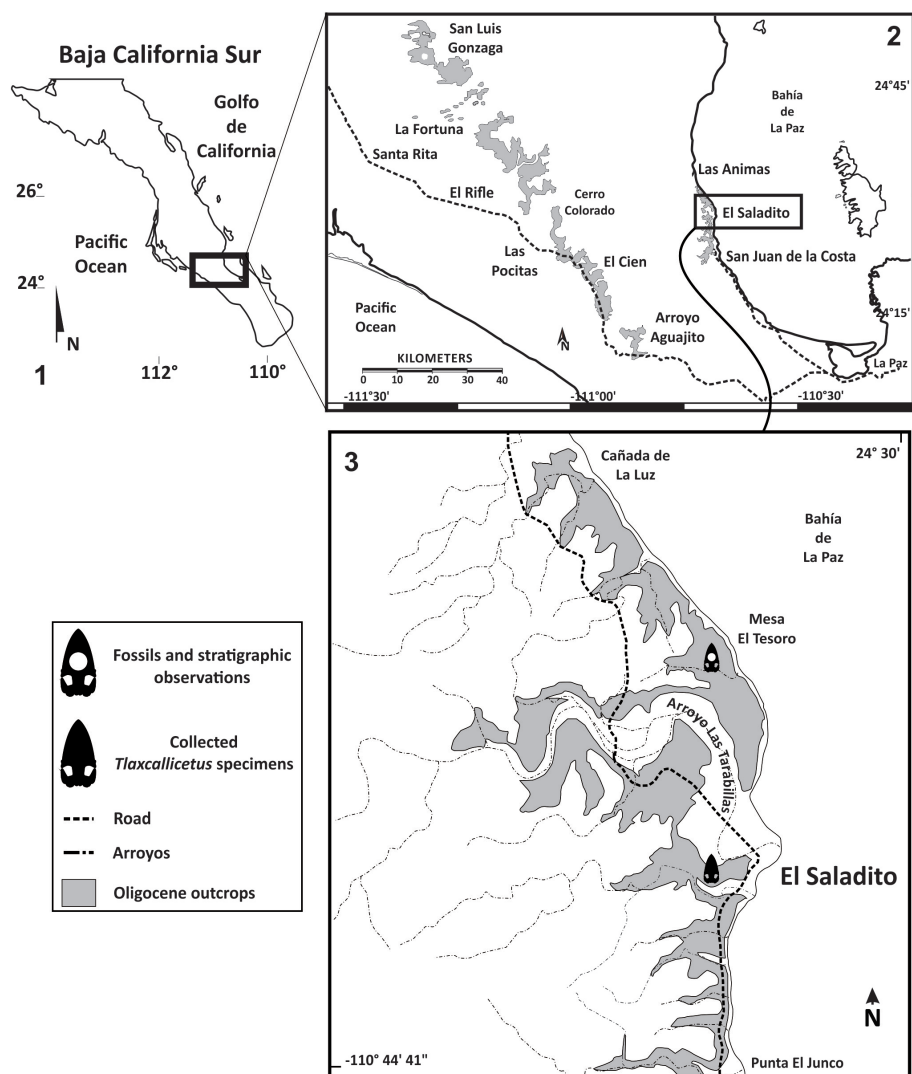


**FIGURE 1.** Map locality, 1) state of Baja California Sur, Mexico; 2) Oligocene outcrops of San Juan Member, El Cien Formation; 3) El Saladito and mesa El Tesoro fossiliferous localities, north to San Juan de la Costa village.

ies support a tropical environment with high productivity (Kim and Barron, 1986; Smith, 1991; Schwennicke, 1994). San Juan Member outcrops range ~23 to 30 Ma based on K/Ar dates using biotite from a tuff bed (Hausback, 1984), diatom biostratigraphy (Kim and Barron, 1986), foraminifera biostratigraphy, zones P21 and P22, and calcareous nannofossils biostratigraphy NP 24/NP 25 zones (Fischer et al., 1995).

On the other hand, cetacean remains are associated with phosphorite beds and considered allochthonous, originally belonging to shallow-water environments (Fischer et al., 1995). In the case of the specimens MU EcSj5/06/31 and MU EcSj5/18/95, stratigraphic data is not available, but field notes document they were collected from the mine spoils at the El Saladito locality. These latter

rocks are a by-product associated with the principal mine source of phosphorite in the zone. The mainly exploited phosphatic bed is called Humboldt bed and many cetacean fossils are associated with it, but it is not the only horizon rich in cetacean fossils. The Humboldt bed is located around 42–44 m in the general stratigraphic column of San Juan Member at San Juan de la Costa (Schwennicke, 1994). The sedimentary matrix removed from MU EcSj5/06/31 and MU EcSj5/18/95 specimens consisted mostly of grey fine sandstone and few siltstone, and it is similar in texture and colour to the matrix of others fossils from the same locality housed in the paleontological collection of MHN-UABCS. It seems the described specimens, MU EcSj5/06/31 and MU EcSj5/18/95, may come from a phosphatic grey fine sandstone layer located

around ~1 m above the Humboldt bed. This idea was put forward based on new observations from the neighbour outcrops at mesa El Tesoro locality (24.47012 N, -110.69381 W), where similar specimens in situ were found in this horizon (Figure 2). Humboldt bed in mesa El Tesoro is easily found due to mining activity and composed of granular phosphorite. A layer of grey laminated mudstone is located over the Humboldt bed, and above it rests the grey phosphatic sandstone bed (Schwennicke, 1994; Fischer et al., 1995). These three horizons have cetacean fossils that include archaic odontocetes, toothed and toothless mysticetes, as well as possibly *Kekenodon*-like animals (Hernández-Cisneros and Tsai, 2016; Hernández-Cisneros et al., 2017). In addition, the Humboldt bed and the laminated mudstone represent shelf deposits under low-oxygen conditions, which are in contact with the grey sandstone that was probably deposited in a transitional zone between offshore and shore face (Schwennicke, 1994). The estimate age for the specimens MU EcSj5/06/31 and MU EcSj5/18/95 is ~27 Ma based on the planktonic foraminifera data correlated to P21 and P22 zones above the Humboldt bed (see Fischer et al., 1995; Berggren et al., 1995).

### SYSTEMATIC PALEONTOLOGY

Order CETACEA Brisson, 1762  
 Clade NEOCETI Fordyce and de Muizon, 2001  
 Suborder MYSTICETI Gray, 1864  
 Infraorder CHAEOMYSTICETI Mitchell, 1989  
 Incertae familiae  
*Tlaxcallicetus*, new genus  
 (Figures 3-9)

zoobank.org/620CDBE7-4B64-4815-A38F-F1CEA9A76958

**Type species.** *Tlaxcallicetus guaycurae*, new species.

**Included species.** *Tlaxcallicetus guaycurae* (MU EcSj5/06/31) new species, late Oligocene, Baja California Sur, Mexico.

**Diagnosis.** Group of stem mysticetes characterized by a massive cranium. Broad supraoccipital with a concave surface and triangular profile (Figure 3); opening of the foramen magnum with an inverted trapezoidal outline; as well a thick zygomatic process, dorsoventrally and mediolaterally (Figure 6). The posterior end of the nuchal crest is elevated in vertical as in basilosaurids (Figure 7). *Tlaxcallicetus* shows the following autapomorphic features: *i*) a periotic with a long and flattened anteroposteriorly compound posterior process (derived feature); *ii*) a head of the periotic (pars

cochlearis, body of the periotic and anterior process) anteroposteriorly compressed and dorsoventrally expanded with ovoid form, in lateral and medial views; *iii*) an anterior process transversally thin like a lamina with an anterodorsal angle prominent as a linguiform outline, which is approximately more than twice the dorsoventral depth size of the pars cochlearis; *iv*) presence of a basioccipital crest anteroposteriorly longest and thick with a similar profile as “J”; *v*) a prominent exoccipital directed posteriorly, and dorsoventrally thick (~50 mm at posterior end) with a semicircular outline in dorsal view; *vi*) and presence of a non-prominent postglenoid process.

*Tlaxcallicetus* mainly differentiates from other described Oligocene stem Mysticeti (Aetiocetidae, Mammalodontidae, Eomysticetidae, and *Sitsqwayk*, *Mauicetus*, *Horopeta*, and *Whakakai*) in a periotic bone with a compound posterior process (posterior processes of bulla and periotic fused) and the ovoid head of the periotic. *Tlaxcallicetus* is interpreted as a chaeomysticete based on the next derived features: a compound posterior process of the periotic; transversally widened intertemporal constriction; and a postglenoid process of the squamosal posteriorly directed in lateral view (Hernández-Cisneros et al., 2017). Thus, *Tlaxcallicetus* is readily distinct from toothed forms (Llanocetidae, Mammalodontidae, Aetiocetidae) but remnant teeth as in eomysticetids is unknown (see Boessenecker and Fordyce, 2015a). It is largely different from Eomysticetidae: in a zygomatic process of squamosal with an inflated and rounded squamosal prominence, as well as a posteriorly divergent basioccipital crest; from *Sitsqwayk cornishorum*, in an opening of the foramen magnum with an inverted trapezoidal outline, presence of a thick basioccipital crest that is laterally directed near to or at right angle to the long axis of the skull; from *Mauicetus parki*, in a deeply concave and broad supraoccipital, a posteriorly divergent basioccipital crest, a periotic with a vertical anterior keel and a reduced suprimeatal area; from *Horopeta umarere* and *Whakakai waipata*, in a deeply concave and broad supraoccipital, an internal acoustic meatus as a single aperture, and a reduced suprimeatal area. *Tlaxcallicetus* shows several plesiomorphic features: a vertical profile of the nuchal crest at the posterior part, a developed superior process of the periotic, an internal acoustic meatus as a single aperture and a presence of a low transverse crest, a straight medial profile of pars cochlearis, and a presence of fovea epitubaria. The latter features make *Tlaxcallicetus* dif-

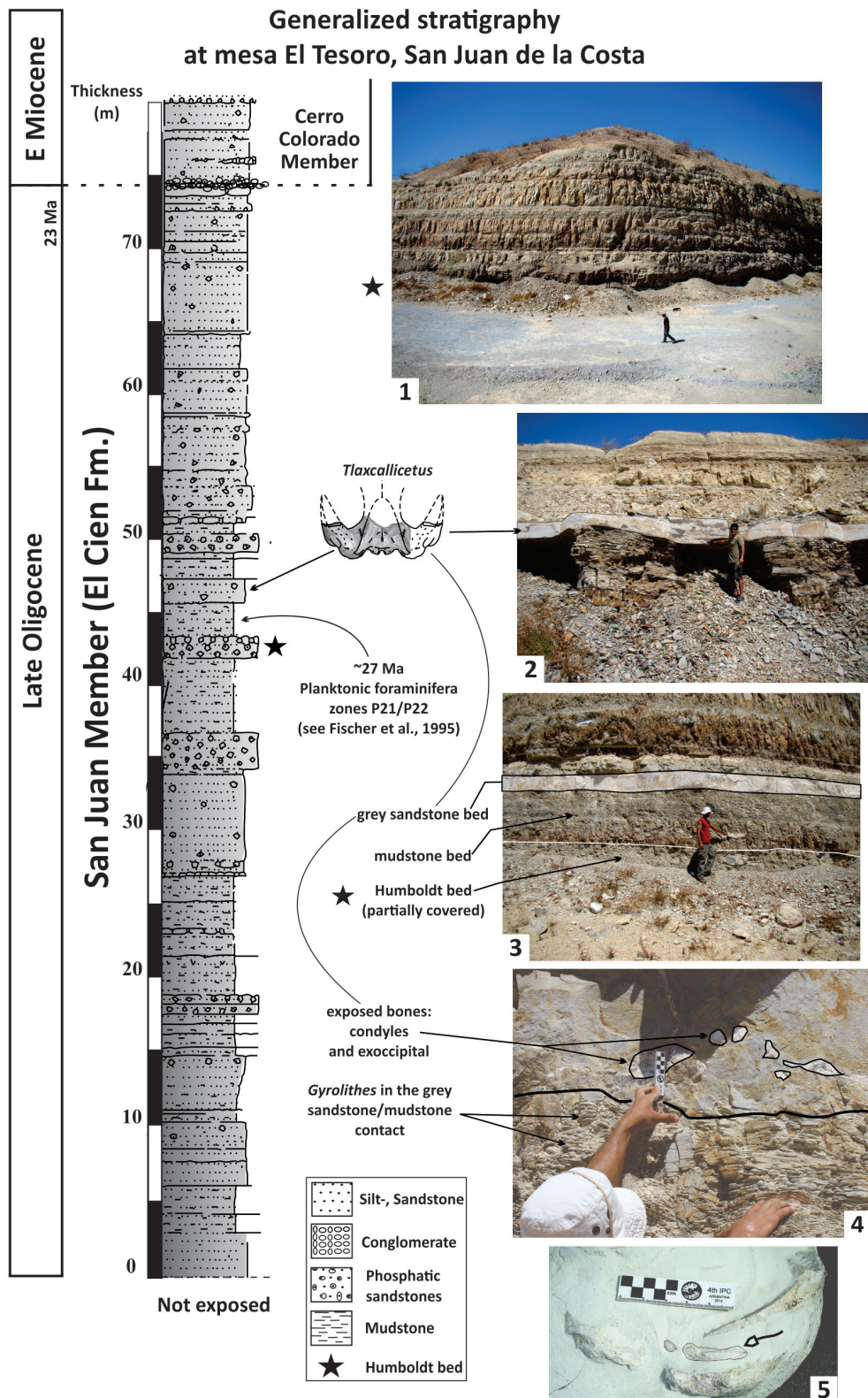


**FIGURE 2.** General stratigraphy and observations at mesa El Tesoro; 1) view of the strata over the mined phosphatic Humboldt bed; 2-3) position of the gray phosphatic sandstone over the Humboldt bed; 4) fossils *Tlaxcallicetus* cf. *guaycurae* *in situ* in the gray phosphatic sandstone and 5) ventral view, left ear region of *Tlaxcallicetus* sp., field observation at mesa El Tesoro.

ferent from the crown Mysticeti (Balaenidae, Cetotheriidae, and Balaenopteroidea, *sensu* Marx and Fordyce [2015]).

**Etymology.** From *tłaxcal-li* (Nahuatl), which means tortilla ('cornbread'), a Mexican iconic food, and refers to Tlaxcala 'the place of tortillas'. From *cetus* (Greek) that enunciates any large sea creature. *Tłaxcal-li* alludes to the transversally thin anterior process of the periotic.

### General Description

**Size and ontogenetic age.** Body length was estimated following Pyenson and Sponberg (2011) equations for stem Mysticeti and stem Balaenopteridae based on the dimension of the bizygomatic width. This latter measure was taken using the preserved dimension from the midline at the condyle to the margin of the preserved zygomatic process in *Tłaxcallicetus guaycurae* (MU EcSj5/06/31). Its estimated total length is between 6.4 and 7.7 m, whereas *Tłaxcallicetus* sp. (MU EcSj5/18/95) is fragmented but comparable in size to *Tłaxcallicetus guaycurae* under incomplete standard dimensions (Hernández-Cisneros et al., 2017). Both specimens are considered as adults because they present well-developed cranial sutures, although they are not completely fused. Juvenile status is discarded because they display a complete occipital ossification (Walsh and Berta, 2011), and occipital condyles without pitted or porous surface exhibiting no associated cartilage (Boessenecker and Fordyce, 2015b).

**Cranial topography.** *Tłaxcallicetus guaycurae* (MU EcSj5/06/31) has the most complete cranium (*sensu* Mead and Fordyce, 2009) but lacks rostrum, frontal, intertemporal region, and postcranial elements. Specimen *Tłaxcallicetus* sp. (MU EcSj5/18/95) includes a broken cranium with partial portions of the posterior middle part of the supraoccipital, left parietal and squamosal, occipital condyles, basioccipital, a fragment of the left thyrohyal bone and broken left ear bones (bullae + periotic). Both specimens show damage due to mining activity, and diagenetic alteration is apparently absent. The main morphological link between *Tłaxcallicetus guaycurae* and *Tłaxcallicetus* sp. is the periotic bone, which is phenetically similar in the ovoid shape of the head of the periotic. Nonetheless, *Tłaxcallicetus* sp. is classified as an undetermined species due to its preservation degree. Although it shows different features (see below) from *Tłaxcallicetus guaycurae*, these are not enough to establish a new species taxon or to classify as one species.

In addition, the posterior process of the periotic in *Tłaxcallicetus* sp. is not preserved. However, a new specimen (in field yet) recently discovered in mesa El Tesoro locality shares a similar morphology to *Tłaxcallicetus* sp. A preliminary identification suggests affinity to *Tłaxcallicetus* sp. and shows a similar periotic (Figures 2.5, 10). The similar ear bone morphology suggests a close relationship between both specimens described here. Note that the ear bones are considered a good diagnostic feature to identify Cetacea (Oishi and Hasegawa, 1994), and the periotic bones are useful for phylogenetic analysis as well as for recognizing groups (Geisler and Luo, 1996; Steeman, 2010).

### *Tłaxcallicetus guaycurae*, new species Figures 3-8

zoobank.org/3B27C833-31FE-4DF7-9929-78E860A1EEF8

**Diagnosis.** The autapomorphic characters that distinguish *Tłaxcallicetus guaycurae* from other known Oligocene archaic chaeomysticetes include: *i*) presence of an external occipital sulcus (new term) on the posterior middle part of the supraoccipital; *ii*) well-developed and deeper dorsal condyloid fossae; *iii*) well-defined supracondylar septum (new term that refers to the prominent elevation of dorsal surface on the middle line of the foramen magnum); *iv*) a prominent exoccipital posteriorly directed farther from the posterior edge of the occipital condyles; *v*) inflated and rounded squamosal prominence; *vi*) posterior end of basioccipital crests transversally aligned to the level of the straight postglenoid process; *vii*) posteriorly exposed ventral surface of the paroccipital process of the exoccipital; *viii*) postglenoid process at same level that the ventral edge of the exoccipital, lateral view; *ix*) half-moon shaped fenestra rotunda; and *x*) a flattened anteroposteriorly compound posterior process.

**Etymology.** The specific name *guaycurae* (Latinized) recognizes the 'Guaycura' indigenous group that lived throughout the municipality of La Paz, Baja California Sur, region where the holotype was found.

**Material.** *Tłaxcallicetus guaycurae* is known only from the holotype, MHN-UABCS\_EcSj5/06/31, which includes a partial cranium without rostrum, mandibles and postcranial bones. The best-preserved fragments of *Tłaxcallicetus guaycurae* include a left broken zygomatic process of squamosal, a well preserved left squamosal fossa, a glenoid fossa, a supraoccipital without apical portion, occipital condyles, left part of the exoccipital, basioccipital, and an almost complete left periotic

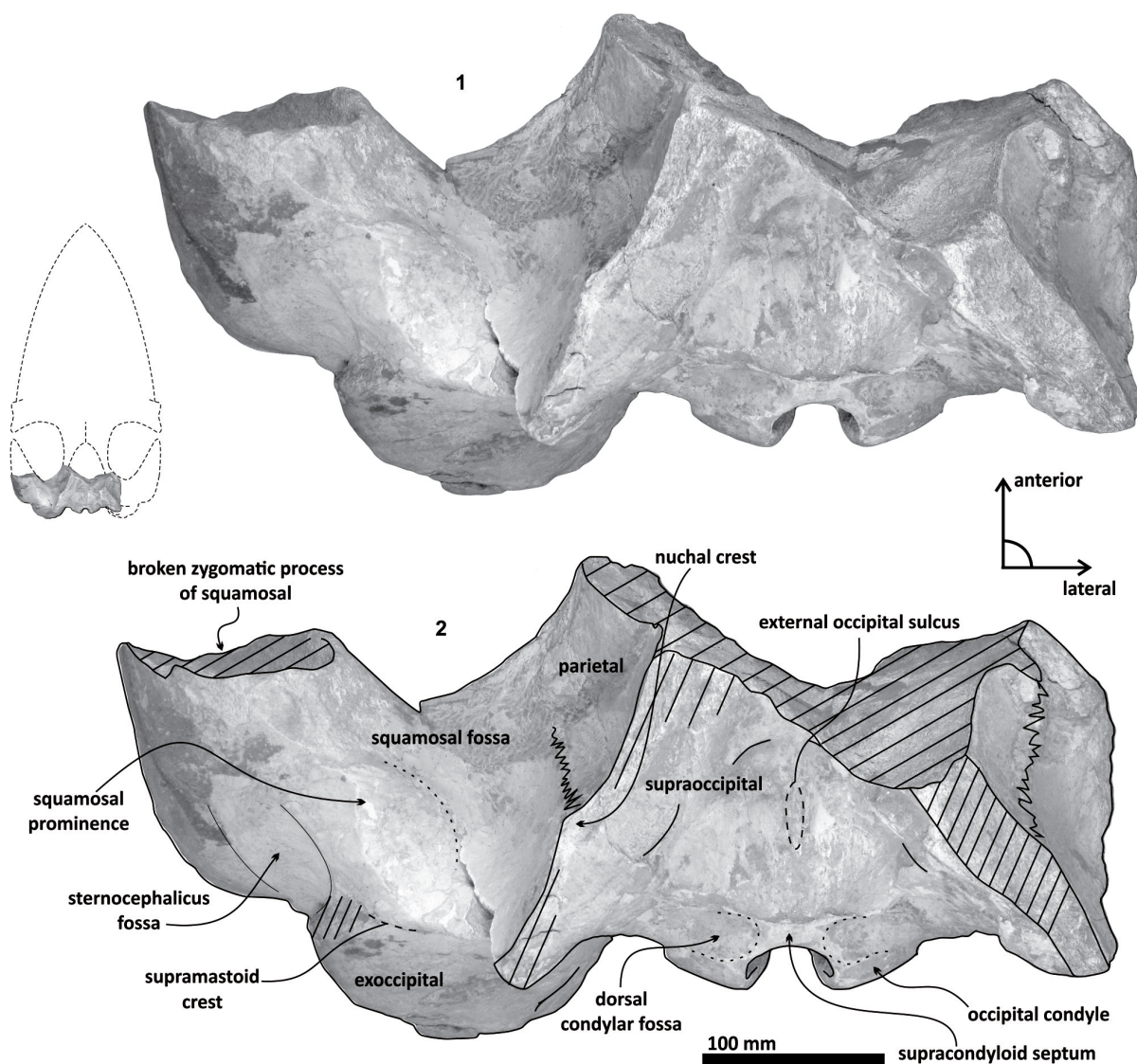


FIGURE 3. *Tlaxcallicetus guaycurae* (MU EcSj5/06/31), cranium, dorsal view.

bone. Specimen was collected by G. Gonzalez-Barba, December 1, 1991.

**Type locality.** El Saladito (mine spoils), San Juan de la Costa, La Paz, Baja California Sur, Mexico (24.43916 N, -110.69512 W). See details in Figure 1.

**Horizon.** From a phosphatic grey fine sandstone bed ~1 m above the Humboldt bed at the general stratigraphic column (Figure 2) of San Juan de la Costa (Schwennicke, 1994).

**Age.** Late Oligocene, ~27 Ma based on the planktonic foraminifera (see above).

### Description

**Parietal.** A small posterior part of parietals is preserved. The surface is concave and fused to the squamosal. No foramina or other important characters are seen (Figures 3, 5, 7). The parietal/squamosal suture obliquely descends over the anterior portion of the squamosal fossa. Its contact with the sphenoid bone is not well defined; the suture is dorsally and posteriorly convex, close to the nuchal crest, and apparently, the parietal forms most of the nuchal crest together with the supraoccipital.

**Supraoccipital.** The apex of the supraoccipital is broken, and the nuchal crests are practically eroded. A small preserved anterior portion suggests that the anteromedial surface of the supraoc-

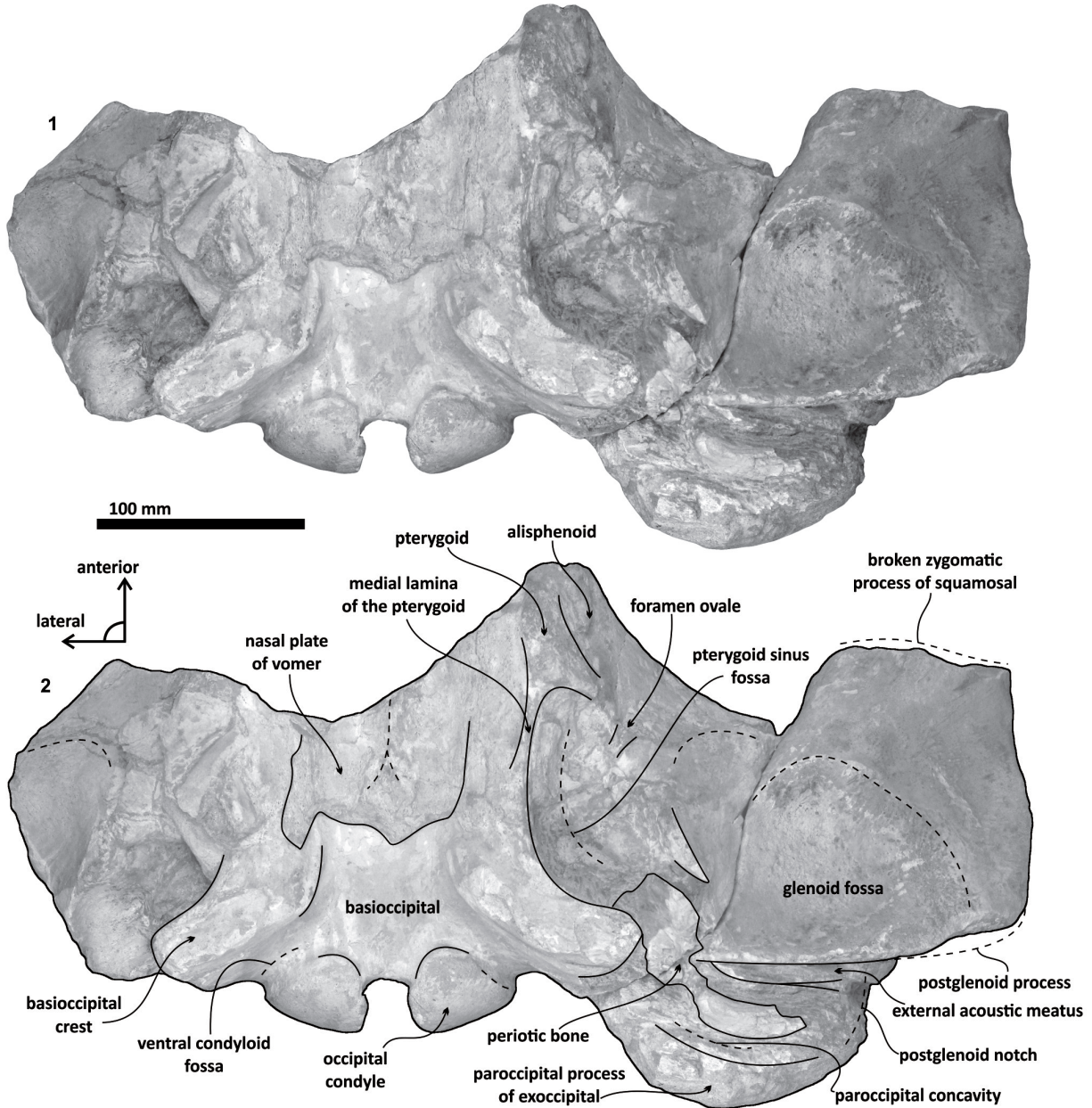


FIGURE 4. *Tlaxcallicetus guaycurae* (MU EcSj5/06/31), cranium, ventral view.

cipital was elevated relative to the posteromedial part, and may have had a triangular profile in dorsal view (Figure 3). The nuchal crest is dorsally convex and ventrally concave on the parietosquamosal surface, and overhangs the squamosal fossa. Its posterior part turns down over the exoccipital/squamosal suture, and an inflexion defines the origin of the eroded supramastoid crest, which extended laterally over the exoccipital/squamosal contact. It does not follow a continuous path over the dorsal surface of the zygomatic process. The

nuchal crest runs posteriorly directed and falls into a vertical profile as in the basilosaurids. The posterior middle part of the supraoccipital is depressed (Figure 6). Its surface is smooth and flat (slightly convex) with a sagittal oval sulcus (external occipital sulcus) in the middle anterior part of the flat surface. The external occipital sulcus is around 5 mm deeper, and is unique for *Tlaxcallicetus guaycurae* (Figure 9.3). No other known mysticete has one. This sulcus is probably a reinforcement of the epaxial muscle for feeding proposes maintaining a

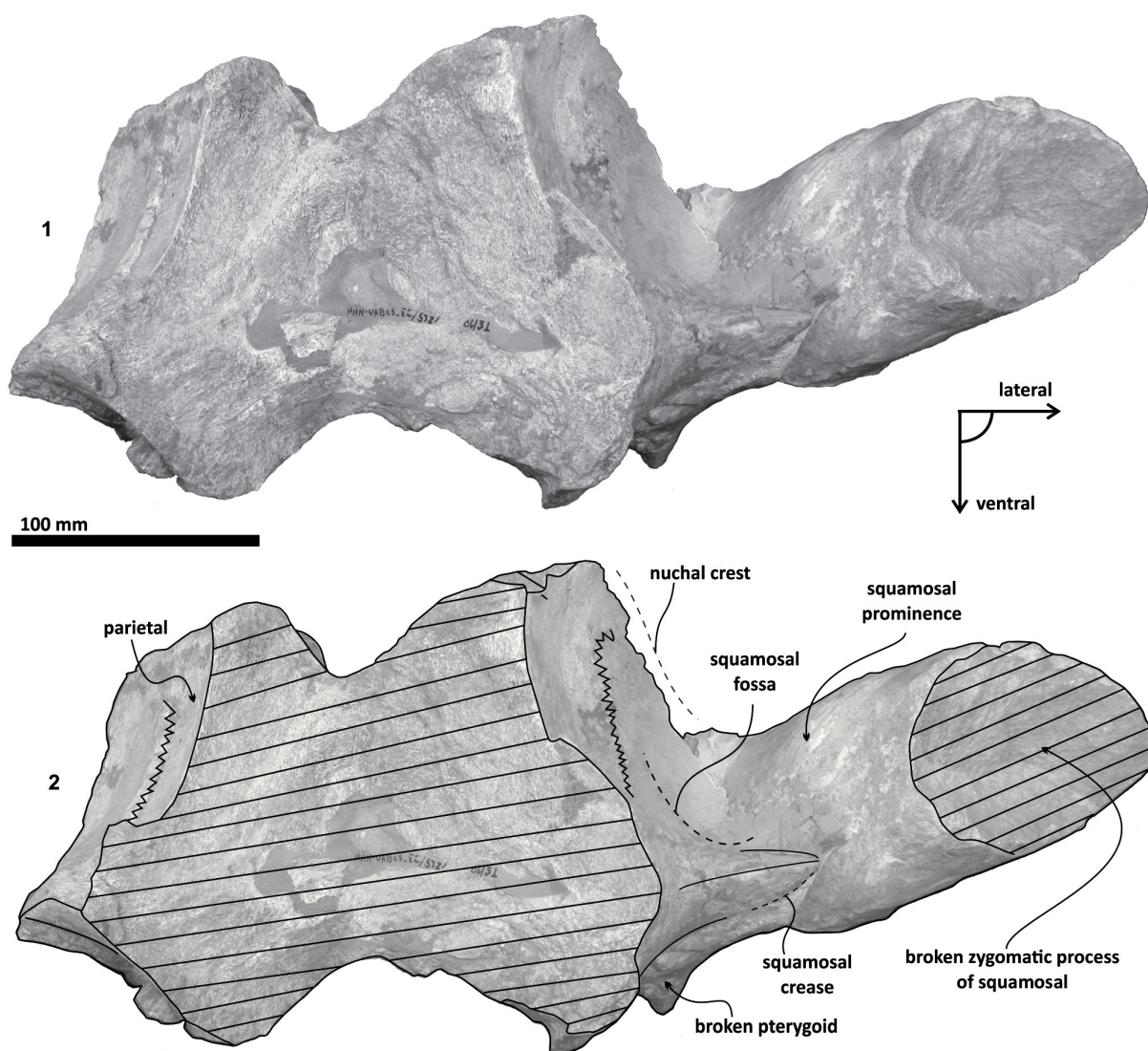


FIGURE 5. *Tlaxcallicetus guaycurae* (MU EcSj5/06/31), cranium, frontal view.

strong atlantooccipital joint associated to the *rectus capitis dorsalis major* and the *rectus capitis dorsalis minor* (see Bouetel, 2005; Evans and de Lahunta, 2013).

**Exoccipital.** Posteriorly, the supraoccipital meets the exoccipital (Figures 3, 6). Dorsal to the occipital condyles, a particularly deep, rounded, and well-developed dorsal condyloid fossa appears. This feature is present in other Oligocene primitive mysticetes as a shallow depression; for example, in eomysticetids (Boessenecker and Fordyce, 2014), or some aetiocetids (Barnes et al., 1995) but apparently, it is also present in many cetaceans and provides a room for movements of the atlas (Mead and Fordyce, 2009). Between the condyloid fossae, a well-defined and prominent supracondy-

lar septum is present. It is not certain if the latter is common in cetaceans with deeper dorsal condyloid fossae; however, a tenuous form of this septum is seen in some fossils (e.g., *Eomysticetus whitmorei*). Laterally, the exoccipital is located posterior to the squamosal; it is prominent and posteriorly directed towards the posterior edge of the occipital condyles. This pronounced extension is dorsoventrally thick (~50 mm at its posterior end). From a dorsal view, it has a semicircular outline, and the dorsal surface is slightly concave. This feature is unique in *Tlaxcallicetus*. Ventrally, the paroccipital process in the exoccipital is thick (~30 mm anteroposterioly) and is exposed posteroventrally. Apparently, its surface has a broad attachment area for the abductor digastric muscle (see El Adli and

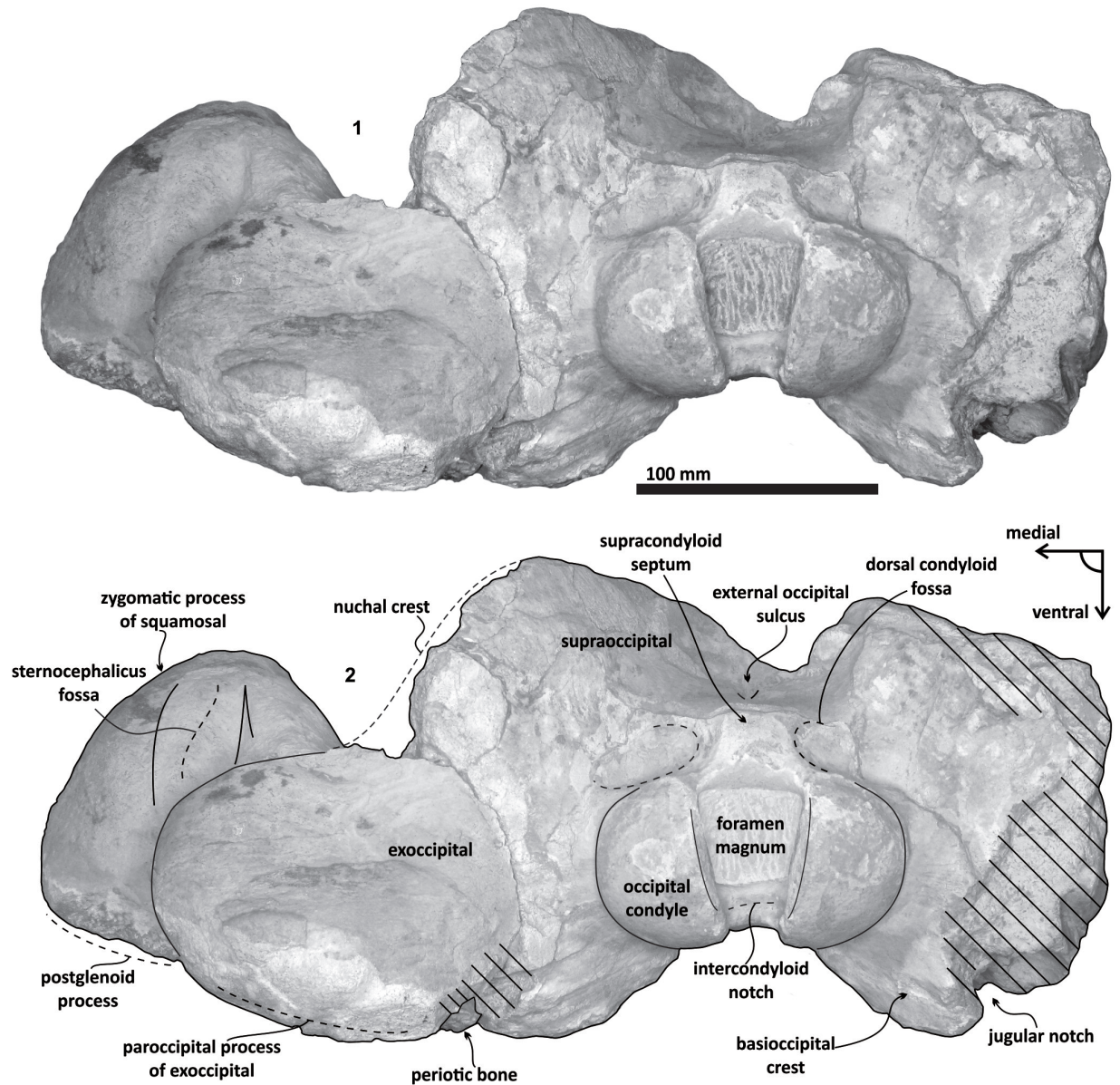


FIGURE 6. *Tlaxcallicetus guaycurae* (MU EcSj5/06/31), cranium, posterior view.

Deméré, 2015). The jugular notch is open widely between the exoccipital and basioccipital crest. A hypoglossal foramen is situated near to the posterior end of the basioccipital crest and opens into the jugular notch.

**Basioccipital.** The basioccipital forms the cranial base (Figure 4)—basilar part (*sensu* Fitzgerald, 2010). It is smooth medially and becomes flat to slightly convex dorsally. Anteriorly, it is fused to the basisphenoid and ventrally overlaps to the posterior end of vomer (nasal plates fragment). Ventrally, the basilar part extends forming a prominent and thick basioccipital crest with a

slightly eroded convex surface. Basioccipital crest is long and bulbous, mediolaterally and dorsoventrally thickened, as in all mysticetes (Fitzgerald, 2010). The crest curves laterally in a right angle at the level of the postglenoid process. The entire crest extends between the middle part of the pterygoid sinus fossa and postglenoid process. Its lateral margin is concave and forms part of the pterygoid sinus fossa, and the blunt apex marginally overhangs the head of the periotic as well as over the periotic fossa. Moreover, the crest is transversally thick, around ~35 mm, near its posterior tip

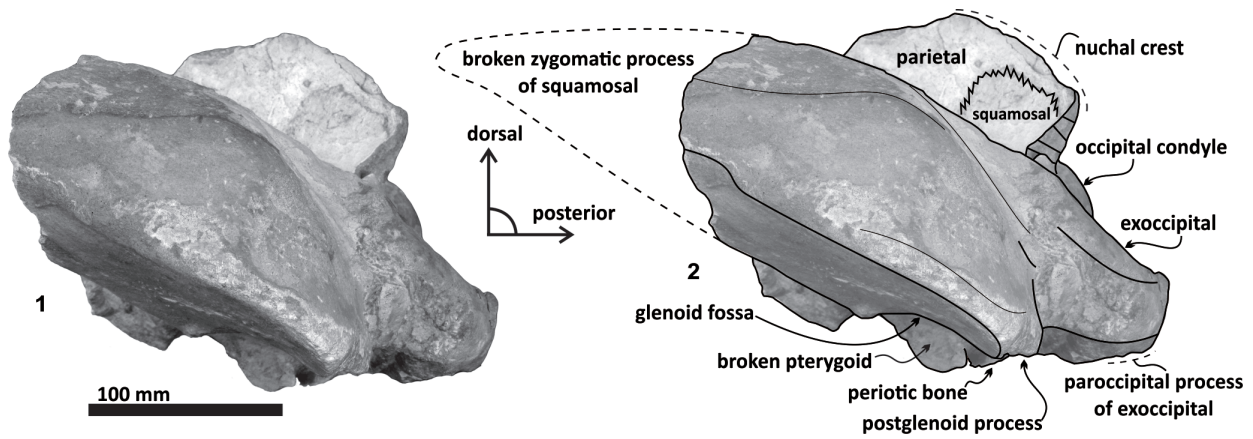


FIGURE 7. *Tlaxcallicetus guaycurae* (MU EcSj5/06/31), cranium, lateral view.

end. This latter feature also distinguishes it from *Tlaxcallicetus* sp.

**Squamosal bone.** The dorsal squamosal surface meets the posterior part of the parietal, and both form the concave space of the squamosal fossa (Figure 3, 5). The fossa is anteroposteriorly short

and transversally broad. A rounded and inflated squamosal prominence rules the lateral surface of the squamosal fossa at the medial part of the base of the zygomatic process of the squamosal. The base of the zygomatic process is transversally wide and posteriorly fused into the exoccipital. The

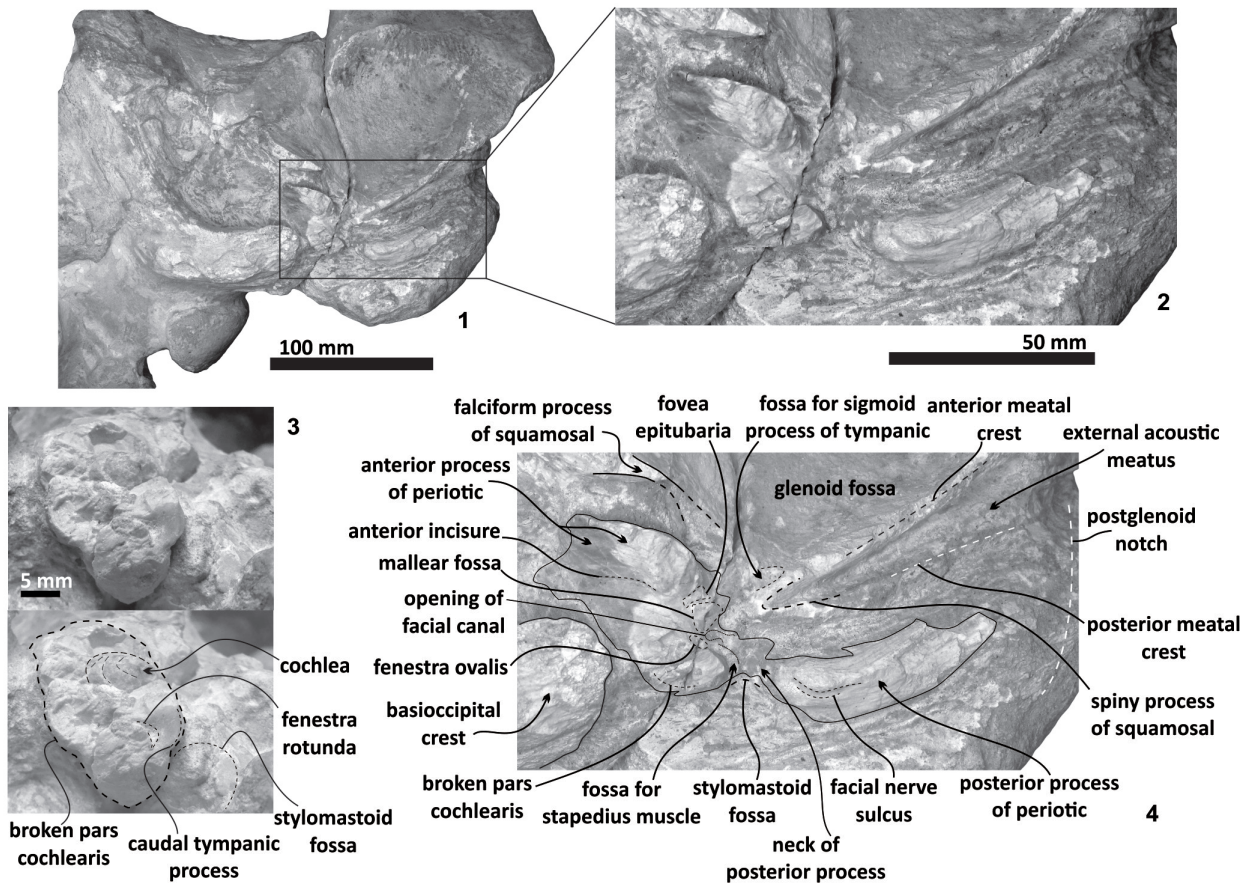
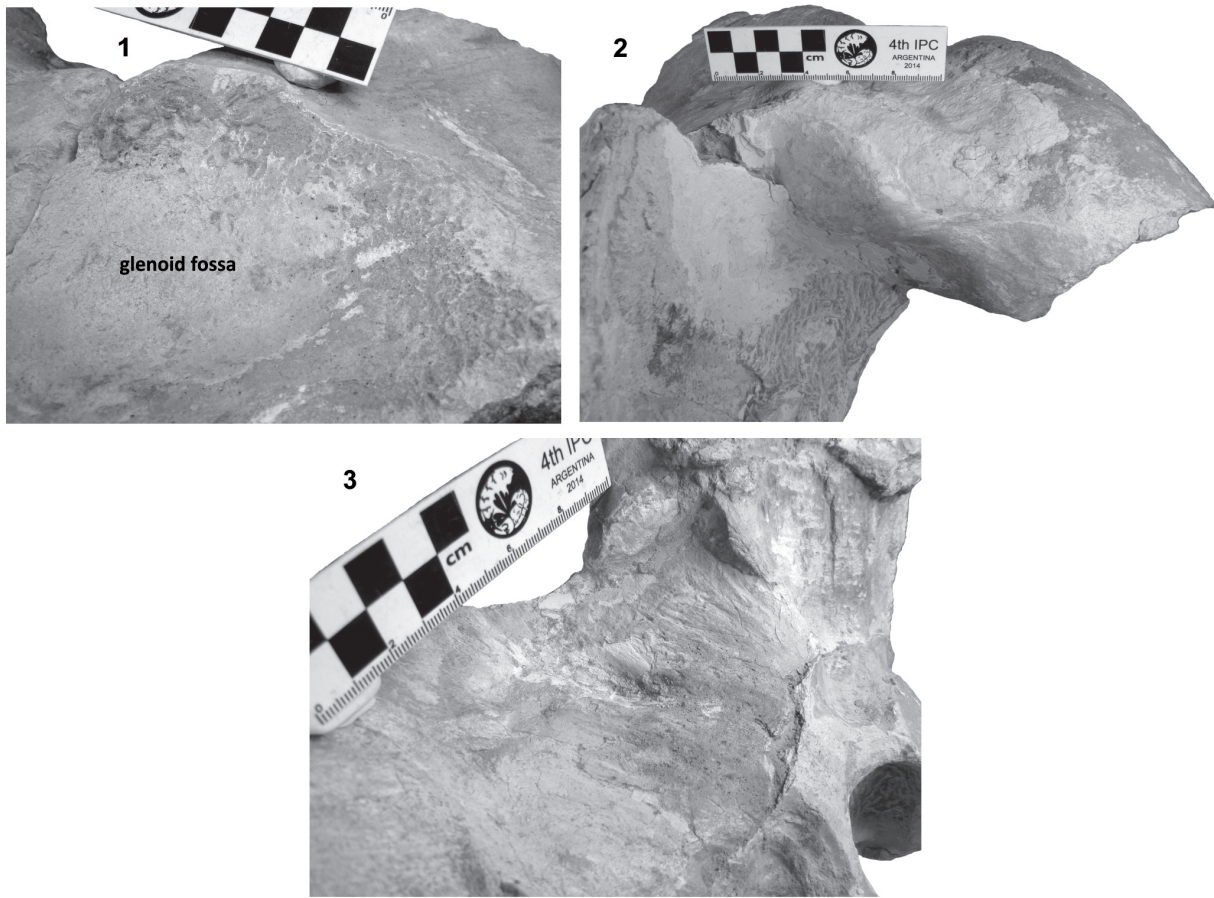


FIGURE 8. *Tlaxcallicetus guaycurae* (MU EcSj5/06/31), ear region (1) with the left periotic bone (2-4), ventral view. Pars cochlearis (3), posteromedial view.



**FIGURE 9.** Detailed features of *Tlaxcallicetus guaycurae* (MU EcSj5/06/31), (1) pitted edge in the glenoid fossa that suggest a fibrocartilaginous joint; (2) inflated and rounded squamosal prominence; (3) external occipital sulcus on the posterior middle part of the supraoccipital.

supramastoid crest is broken, it is laterally directed and continues between the nuchal crest and exoccipital joint but is not present over the zygomatic process. Dorsolaterally and next to the squamosal prominence occurs a broad sternocephalic fossa with a flat to slightly convex surface. Its oval area is limited by a blunt and thin ridge. Ventrally, the postglenoid process is exposed on the posterolateral margin of the base of zygomatic process. The apex of the zygomatic process is broken but in the anterior view can be seen a round transverse section that suggests a conical shape (Figure 5). The left glenoid fossa is broad and concave. Its outline is nearly semicircular with the anterolateral margin marked by a visible pitted surface (Figure 9.1). These pits could imply the presence of a possible non-synovial and fibrocartilaginous joint, similar to the one in balaenopterids (Lambertsen et al., 1995). Posteriorly, the glenoid fossa is limited by a perpendicular and straight postglenoid process (relative to the sagittal axis), which is aligned to the

rear of the basioccipital crest. The postglenoid process is relatively thick in lateral view and posteroventrally directed. Thus, it is different from the anteriorly curving postglenoid process present in archaic tooth-bearing mysticetes as the aetiocetids (Barnes et al., 1995) or the eomysticetids (Sanders and Barnes, 2002a, 2002b, Boessenecker and Fordyce, 2015a, 2015b). Also, it is small and not prominent ventrally or posteriorly, and is aligned ventrally to the paroccipital process of the exoccipital. Posteriorly to the postglenoid process, a broad postglenoid notch opens. Inside, the external acoustic meatus is mediolaterally long and relatively narrow anteroposteriorly, between the anterior and posterior meatal crests of the squamosal. Medially to the glenoid fossa, the falciform process is broken. The pterygoid sinus fossa is a deep cavity with an ovoid shape and anterolaterally, the foramen ovale canal crosses the pterygoid sinus fossa. A small and indistinct fossa for sigmoid process is also present near the spiny process of the

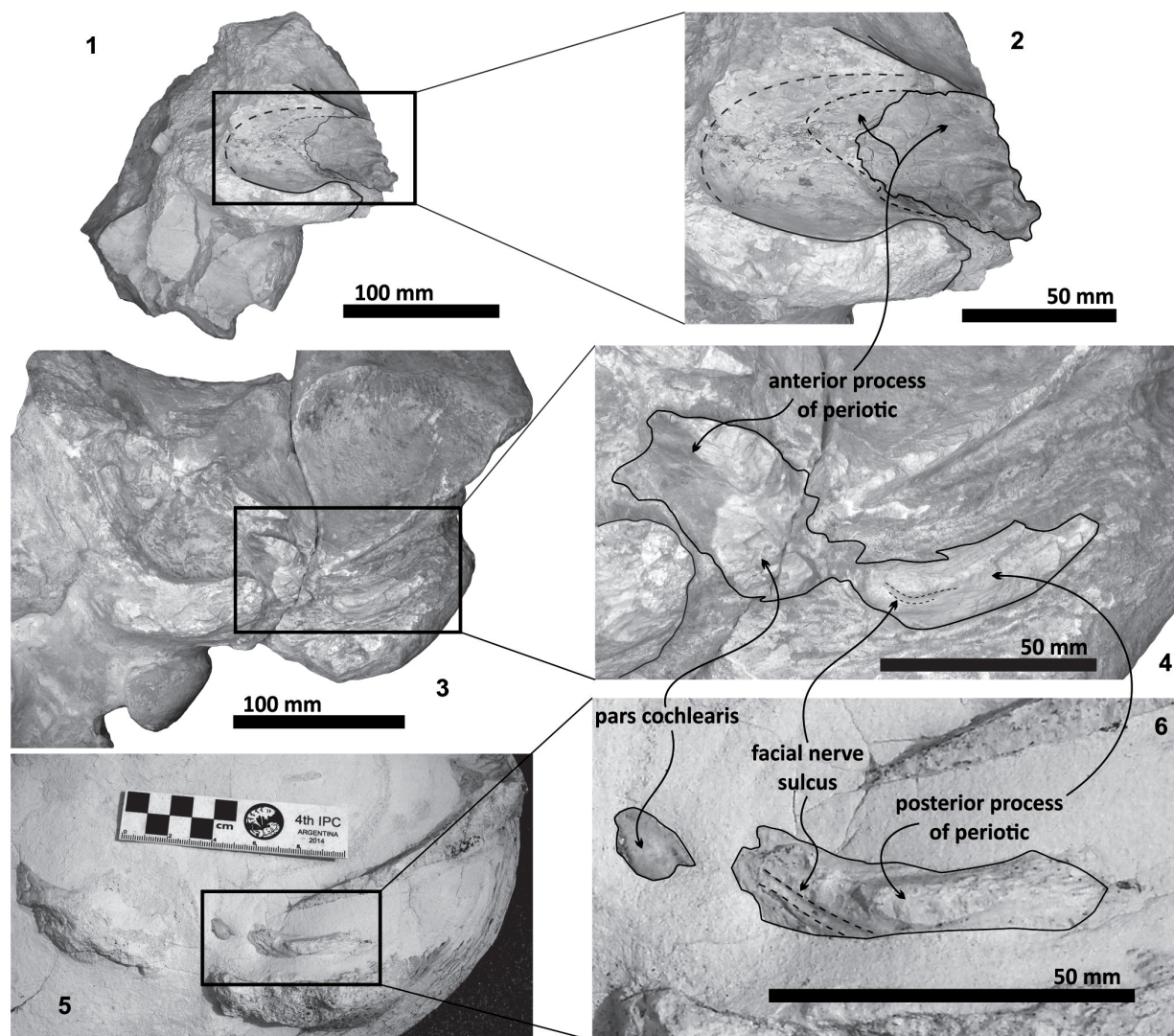


**FIGURE 10.** Ear region and left periotic comparison between *Tlaxcallicetus* species, ventral view. *Tlaxcallicetus* sp. (MU EcSj5/18/95) (1-2), *Tlaxcallicetus guaycurae* (MU EcSj5/06/31) (3-4), and specimen found at mesa El Tesoro, *Tlaxcallicetus* sp., field observation (5-6).

squamosal. The left periotic is *in situ* and practically complete within the periotic fossa.

**Vomer/ Alisphenoid/ Pterygoid.** Some fragments of the alisphenoid, vomer, and pterygoid are preserved. The pterygoid is lateral to the posterior end of the vomer (nasal plates) but is broken. Apparently, the pterygoid forms part of the foramen ovale, and a thin medial lamina of the pterygoid is preserved. Alisphenoid is fused laterally to the pterygoid and represents just a portion of the ventral surface of the braincase. The nasal plates of vomer are wide transversally and are divided by an eroded vomerine crest.

**Periotic.** The periotic is the best diagnostic feature of *Tlaxcallicetus*. In *Tlaxcallicetus guaycurae*, the

periotic is basically complete, but the dorsal surface (internal acoustic meatus, suprameatal area, superior process, the aperture to the vestibular aqueduct, and the cochlear aqueduct) is not visible (Figure 8). However, it is anatomically similar to the *Tlaxcallicetus* sp. (MU EcSj5/18/95), left periotic (Figure 10). The anterior process of the periotic is transversally narrow (~10.5 mm as maximum at the base near the fovea epituvaria), and very thin dorsally. The anterior keel is vertical. The anterodorsal angle and the anteroventral angle are broken. In the posteriomedial wall of the anterior process and anterior to pars cochlearis, a marked anterior incisure is present. Ventrally, the incisural flange is eroded. Posteriorly to the broken antero-

ventral angle, a rectangular and narrow fovea epitubaria appears. The adjacent malleolar fossa is poorly preserved but looks rounded, concave with a well-defined margin, and oriented posteroventrally. The lateral tuberosity is not complete but the fragments suggest that it is blunt and indistinct; posteriorly, the fossa incudis is eroded. The fenestra ovalis is broken and nearly elliptical, oriented ventrally and located anteromedial to the distal opening of the facial canal. The fossa for the stapedius muscle is anteroposteriorly long, finishing in the stylomastoid fossa. The pars cochlearis is broken in its ventromedial surface, without evidence of an anterointernal angle or a median promontorial groove. The cochlea is exposed ventrally. Posteriorly, the fenestra rotunda is preserved as a half-moon groove and ventrally, the caudal tympanic process has a low profile with a blunt margin (Figure 8.3). The head of the periotic is connected by a cylindrical neck to the posterior process. On the dorsomedial surface between the posterior part of the pars cochlearis and the posterior process, a prominent depression of the stylomastoid fossa is present. The tympanic and periotic posterior processes are fused and form a compound posterior process oriented in a right angle to the axis of the anterior process. It is flattened anteroposteriorly. Near the neck and closer to the posterior margin of the posterior process, a transversally short facial nerve sulcus appears.

*Tlaxcallicetus* sp.  
Figures 11-21

**Diagnosis.** *Tlaxcallicetus* sp. is different from others known Oligocene archaic chaeomysticetes (eomysticetids, *Sitsqwayk cornishorum*, *Mauicetus parki*, *Whakakai waipata*, and *Horopeta umarere*) because it presents a long, thick, and posterolaterally directed J-shaped basioccipital crest. It also has an inverted trapezoidal foramen magnum opening, a periotic ovoid head with a transversally narrow anterior process similar to a lamina, and a prominent anterodorsal angle. *Tlaxcallicetus* sp. differs from *Tlaxcallicetus guaycurae* in the following autapomorphic features: a slender basioccipital crests (~22.5 mm width near its posterior end) directed posterolaterally in obtuse angle  $>90^\circ$  and aligned to the medial part of the paroccipital process of the exoccipital. Moreover, the plain surface behind the foramen magnum suggests that it lacks an external occipital sulcus, and also lacks a dorsal condyloid fossa and a supracondylar septum. However, both specimens share general features, but the main observable autapomorphic feature is the presence of a periotic ovoid head with a transversely thin anterior process.

**Material.** MHN-UABCS\_EcSj5/18/95, partial cranium with both broken left periotic and bulla, and fragment of left thyrohyal and fragmentary bones. Collected by G. Gonzalez-Barba, May 4, 1994.

**Type locality, horizon and age.** The same as *Tlaxcallicetus guaycurae* (see above).

### Description

**Skull.** A fragment of the cranium is preserved as well as a piece of the hyoid bone (left thyrohyal).

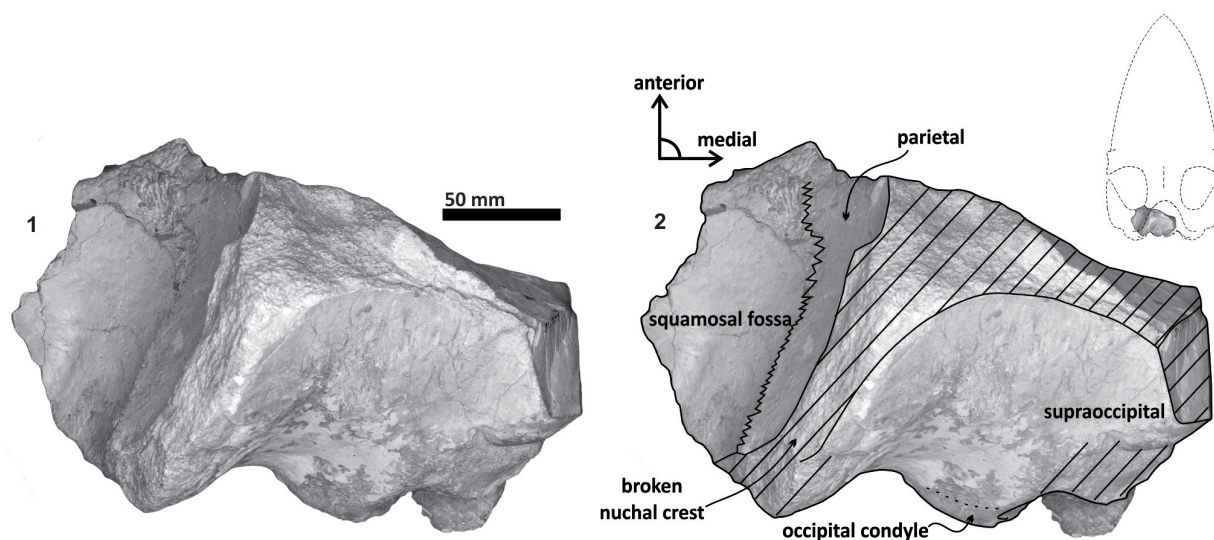


FIGURE 11. *Tlaxcallicetus* sp. (MU EcSj5/18/95), cranium, dorsal view.

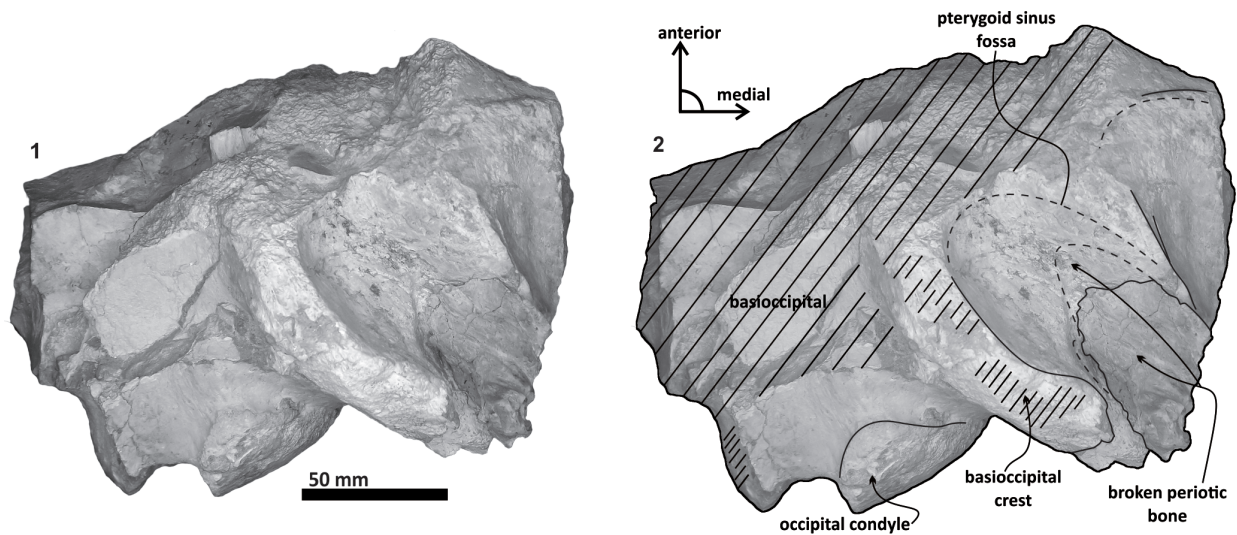


FIGURE 12. *Tlaxcallicetus* sp. (MU EcSj5/18/95), cranium, ventral view.

*Tlaxcallicetus* sp. partial cranium's size is comparable to *Tlaxcallicetus guaycurae*. The fragment displays a dorsal posterior part of the supraoccipital, a fragmentary posterior exoccipital piece, an incomplete ventral basioccipital as well as a fragment of the left ear. From a lateral view (left side), fractions of the parietal and the squamosal can be observed (Figure 11). The supraoccipital piece is smooth with a flat to slightly convex surface, and presents a concave profile from a posterior stand-up point. The incomplete squamosal fossa in *Tlaxcallicetus* sp. is similar to the anteroposteriorly short and transversally broad squamosal fossa of *Tlaxcallicetus guaycurae*. The parietal/squamosal suture is the same as in the *Tlaxcallicetus guaycurae*, and

the broken nuchal crest has a vertical profile in the rear. Posteriorly, the supraoccipital fuses with the exoccipital, and lacks a well-defined supracondylar septum. The left occipital condyle is relatively thick (37.5 mm). Under the occipital condyle, the exoccipital flows into the left basioccipital crest, and the jugular notch is more or less conserved. The basioccipital is mostly broken. Only a long and narrow left basioccipital crest with an eroded surface is preserved. Anteromedially, the crest forms the margin of the broken pterygoid sinus fossa. The apex of the basioccipital crest is bulbous and posterolaterally extends in an obtuse angle  $>90^\circ$ . The pterygoid sinus fossa is deep but anteriorly incomplete. The foramen ovale is not preserved (Figure

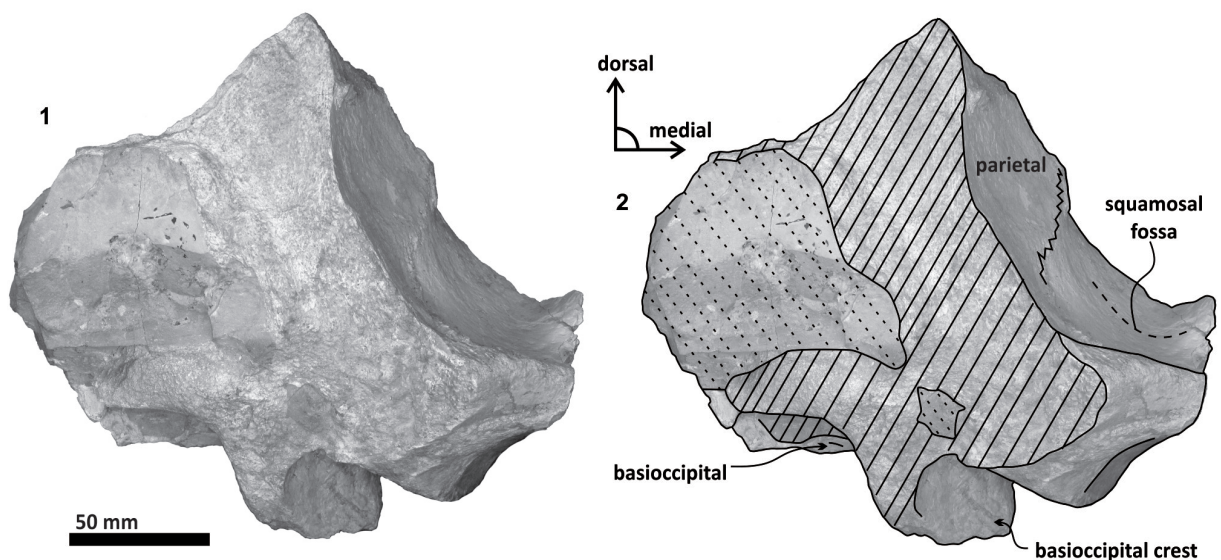


FIGURE 13. *Tlaxcallicetus* sp. (MU EcSj5/18/95), cranium, frontal view.

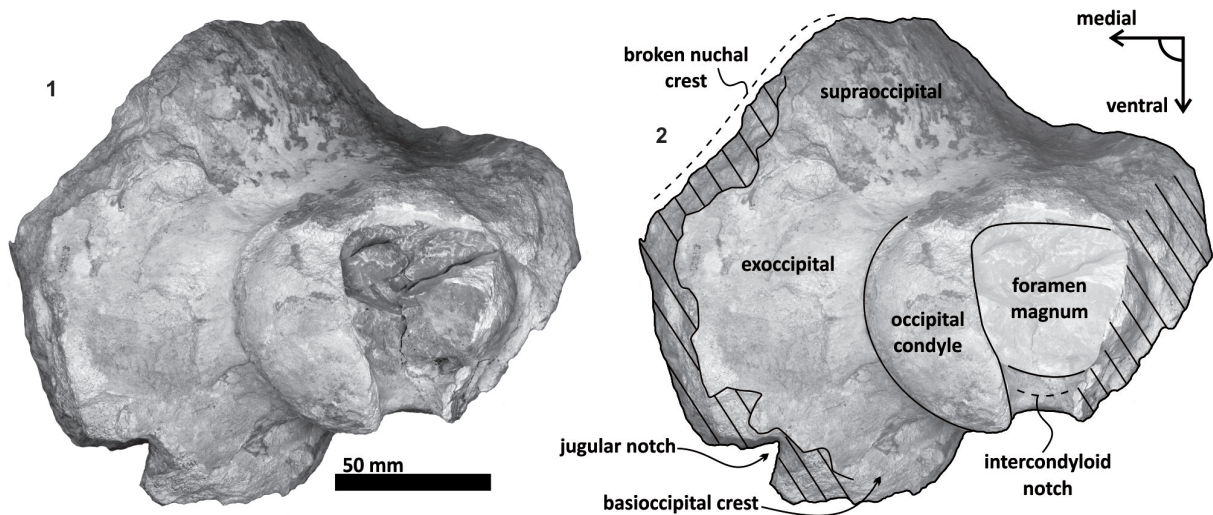


FIGURE 14. *Tlaxcallicetus* sp. (MU EcSj5/18/95), cranium, posterior view.

12), and the falciform process is broken.

**Periotic.** Only a fragment of the left periotic is preserved including a piece of the pars cochlearis, the body of periotic, and the anterior process (Figures 16-18). The head of the periotic has an ovoid shape, anteroposteriorly compressed and dorsoventrally deep. It rests on the periotic fossa and apparently was not firmly ankylosed to the squamosal. However, the linguiform anterodorsal angle is close to the squamosal wall through a thin lamina of bone. The anterior process is dorsoventrally deep (total estimate ~75 mm); more than twice the

depth of the pars cochlearis in *Whakakai waipata*, *Horopeta umarere*, and *Mauicetus parki*. It constitutes a transversally thin lamina (between ~10.5 mm at the base and ~0.5 mm on the top). The anterior process has an ovoid outline with a vertical anterior keel. Both, the anterodorsal angle and the anteroventral angle are broken, and nearly all of the superior process is eroded. The anterior incisure marks the limit between the pars cochlearis and the anterior process, and is slightly vertical. Above of the anterior incisure a small hiatus Fallopii is present. From a lateral view, the periotic

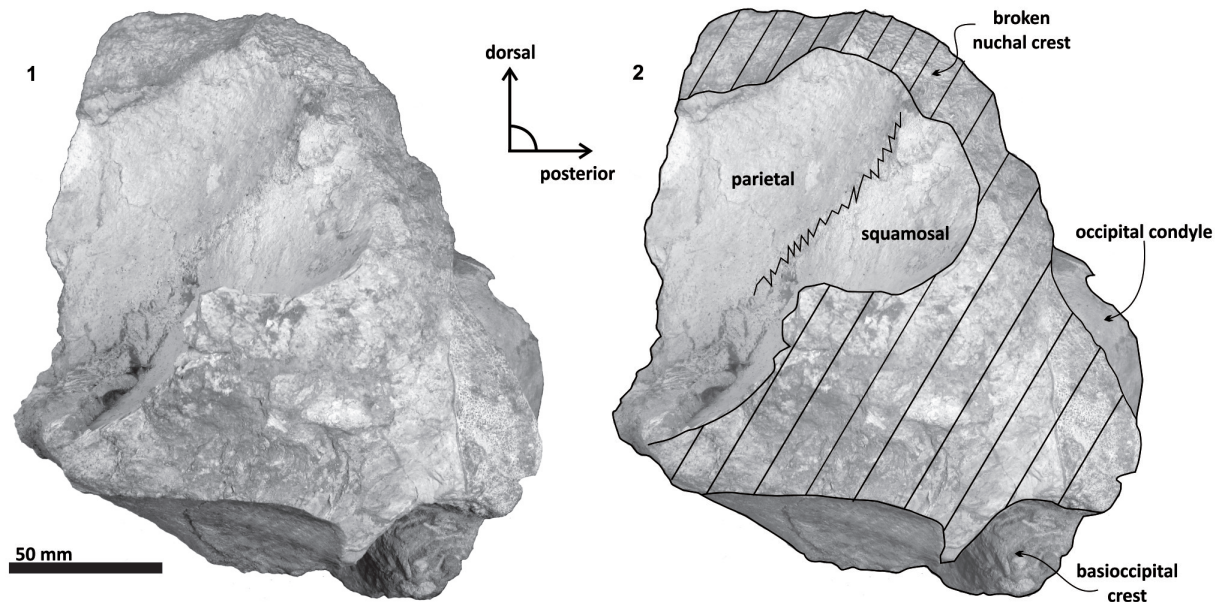
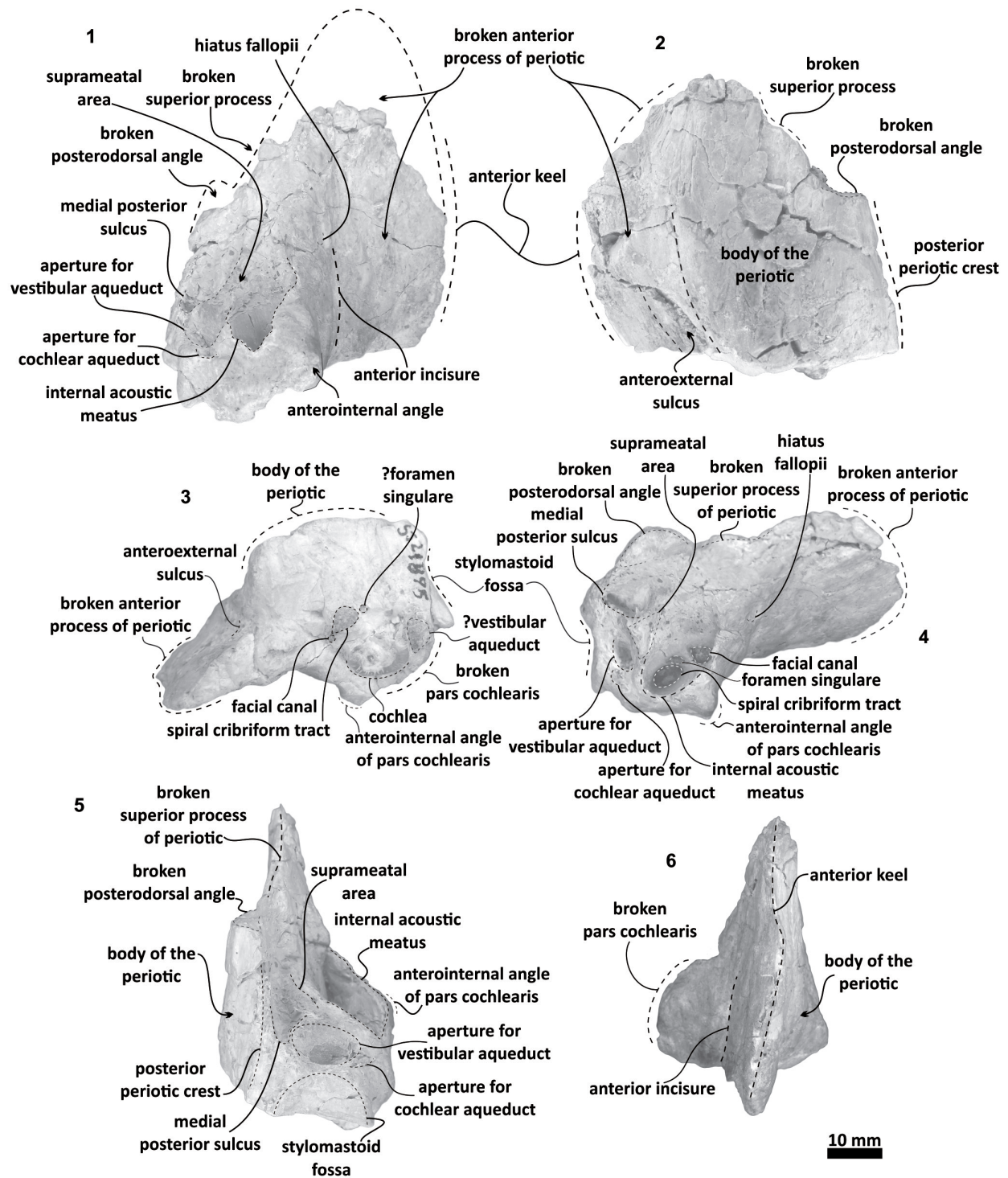
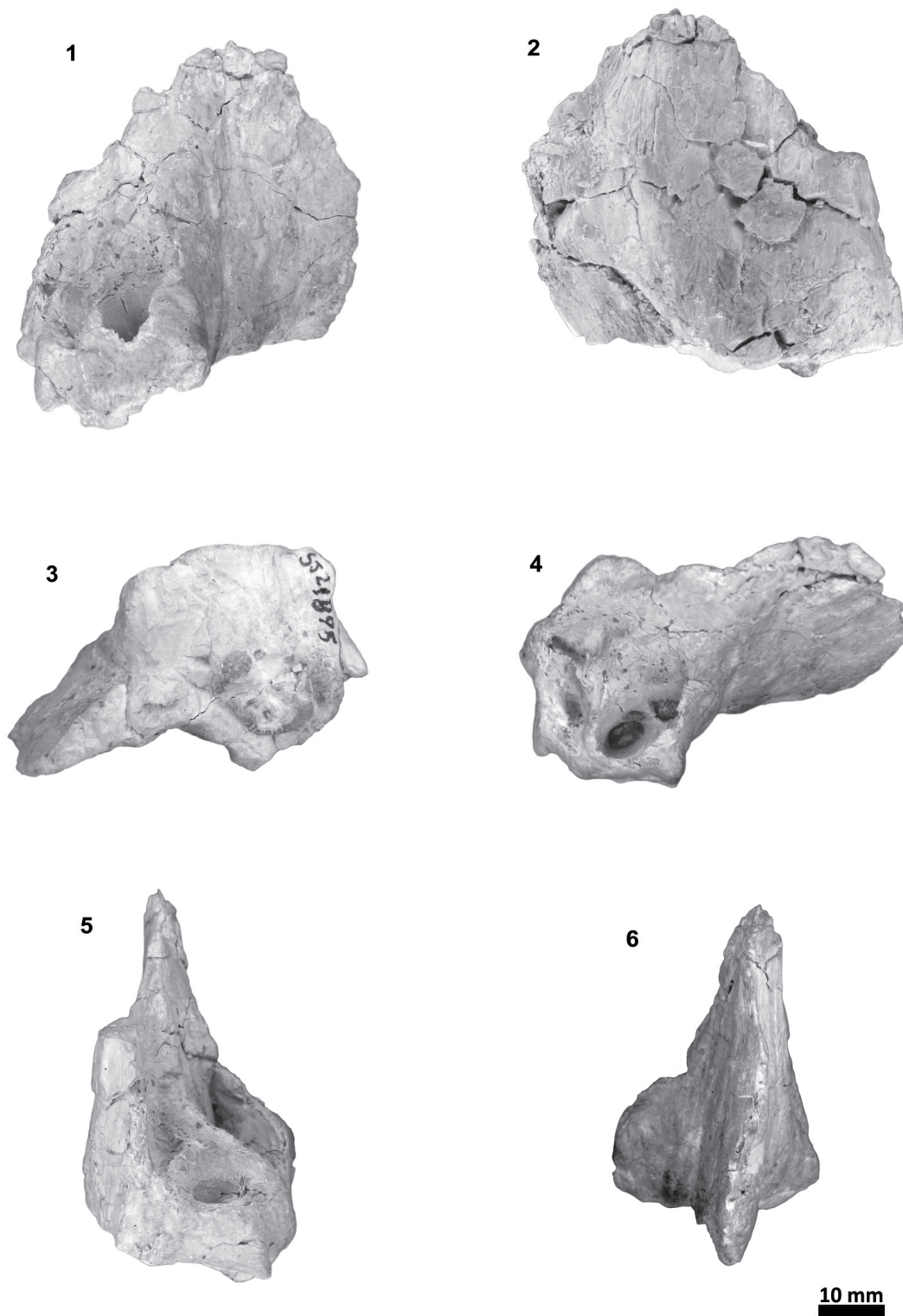


FIGURE 15. *Tlaxcallicetus* sp. (MU EcSj5/18/95), cranium, lateral view.



**FIGURE 16.** Left periotic with anatomical terms, *Traxcallicetus* sp. (MU EcSj5/18/95), medial (1), lateral (2), ventral (3), dorsal (4), posterior (5), and anterior (6) views.



**FIGURE 17.** Left periotic, *Tlaxcallicetus* sp. (MU EcSj5/18/95), medial (1), lateral (2), ventral (3), dorsal (4), posterior (5), and anterior (6) views.

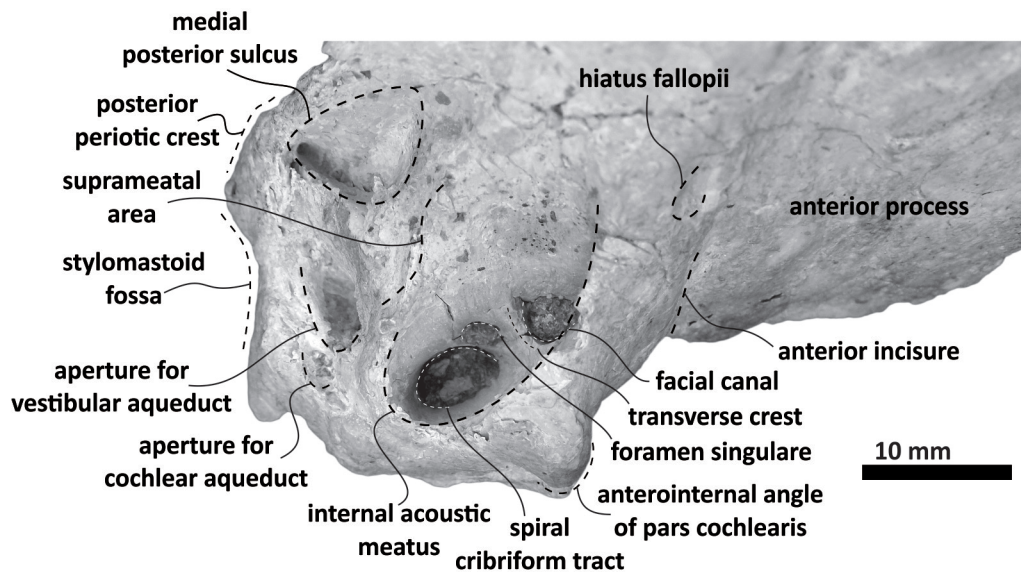


**FIGURE 18.** Left periotic, *Tlaxcallicetus* sp. (MU EcSj5/18/95), closer view of internal acoustic meatus, dorsal view.

body's wall surface is smooth with some vertical small creases near the broad and indistinct antero-external sulcus. The pars cochlearis has a square-rectangular outline with a prominent and blunt anterointernal angle (Figure 16.4, 17.4). The suprameatal area is small and compressed half-way through the internal acoustic meatus, the aperture for vestibular aqueduct, and the medial posterior sulcus. The internal acoustic meatus is anterolaterally directed, oval, and deep, and its anterior margin is overhanging the facial canal. The spiral cribriform tract is a broad opening in the bottom of the internal acoustic meatus. On its lateral wall a stepped foramen singulare, as well as a medium-size facial canal are present. The former is isolated by a low transverse crest. On the posterior surface of the pars cochlearis, an oval aperture for vestibular aqueduct can be observed. Also, another medially minuscule aperture of the cochlear aqueduct is present. Below to the broken posterodorsal angle, a broad medial posterior sulcus is present. On the posterior margin of the pars cochlearis, an incomplete stylomastoid fossa is preserved as a depressed surface.

**Bulla.** Only the left bulla is preserved, and diagnostic details from the dorsal region are missing (Figure 19-20). It is compressed dorsoventrally. In a dorsal view, the bulla has a rectangular-ovoid profile with a straight medial margin, and its anterior border obliquely truncated. The tympanic cavity extends anteroposteriorly. The involucrum is dorsoventrally thick posteriorly and becomes narrow

anteriorly; with fine creases covering its middle part. Medially, the involucrum is posteriorly bulbous with a low anterior portion separated by a step. The involucral ridge extends anteroposteriorly closer to the ventral margin. From a ventral view, it meets the medial edge of the bulla. Dorsally, the base of the inner posterior pedicle is broken and located near the posterior edge. The outer lip is broken. From a ventral view, the outer posterior and inner posterior prominences are not well defined and are separated by an interprominental notch; a shallow median furrow extends from it.

**Thyrohyoid.** The proximal portion of the left thyrohyoid is preserved (Figure 21). In its cross section, it is cylindrical and thick. The anterior end was attached (not fused) to the posterolateral face of the basihyoid. This was inferred based on the oval pitted surface of a possible cartilaginous joint.

## PHYLOGENETIC ANALYSIS

As a result of the cladistic analysis two consensus trees were obtained: the first is a consensus tree from 260 parsimonious trees under equal weights, and the second is a result from three parsimonious trees under implied weights,  $k=6$  (Figure 22). Both consensus trees were simplified focused on the *Tlaxcallicetus*' position. For a more complete analysis on Mysticeti phylogeny, see Marx and Fordyce (2015). Total characters coded for *Tlaxcallicetus guaycurae* represent 33.8% (92/272) of the total matrix and for *Tlaxcallicetus* sp. are 34.9% (95/272).

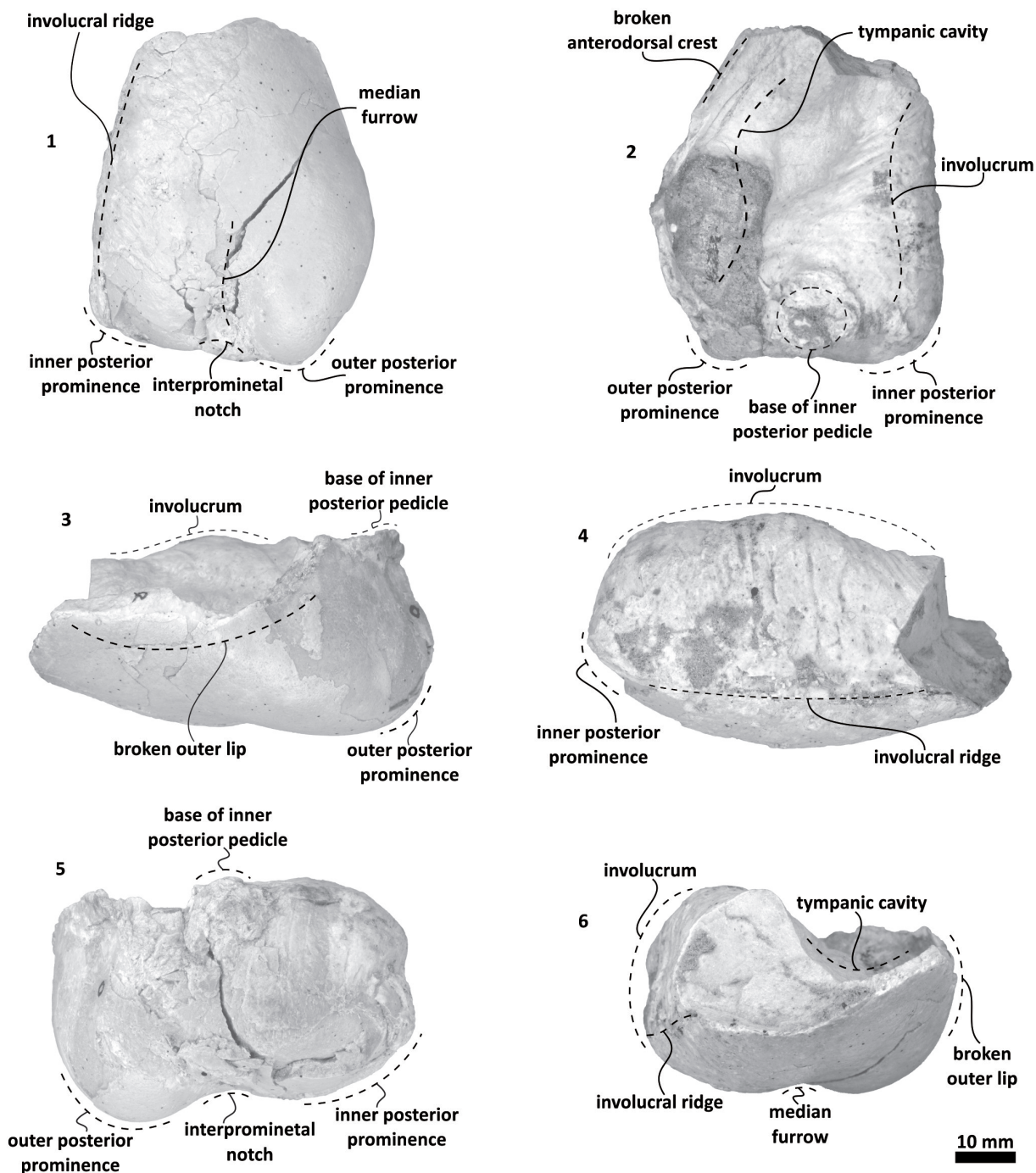


**FIGURE 19.** Left bulla with anatomical terms, *Tlaxcallicetus* sp. (MU EcSj5/18/95), ventral (1), dorsal (2), lateral (3), medial (4), posterior (5), and anterior (6) views.

*Tlaxcallicetus* had low support as a taxon under equal weights (37%) and is poorly supported under implied weights (57%). Furthermore, *Tlaxcallicetus*' phyletic relation is constant in both trees as a sister taxon between *Sitsqwayk* and Eomysticetidae but lies within different polytomies.

Although it shares a same branch with *Sitsqwayk* under implied weights, this can be considered as an artefact arrangement (see Congreve and Lamsdell, 2016). This branch is supported by two non-homoplasious characters: straight and non-prominent outline of the postglenoid process in an ante-

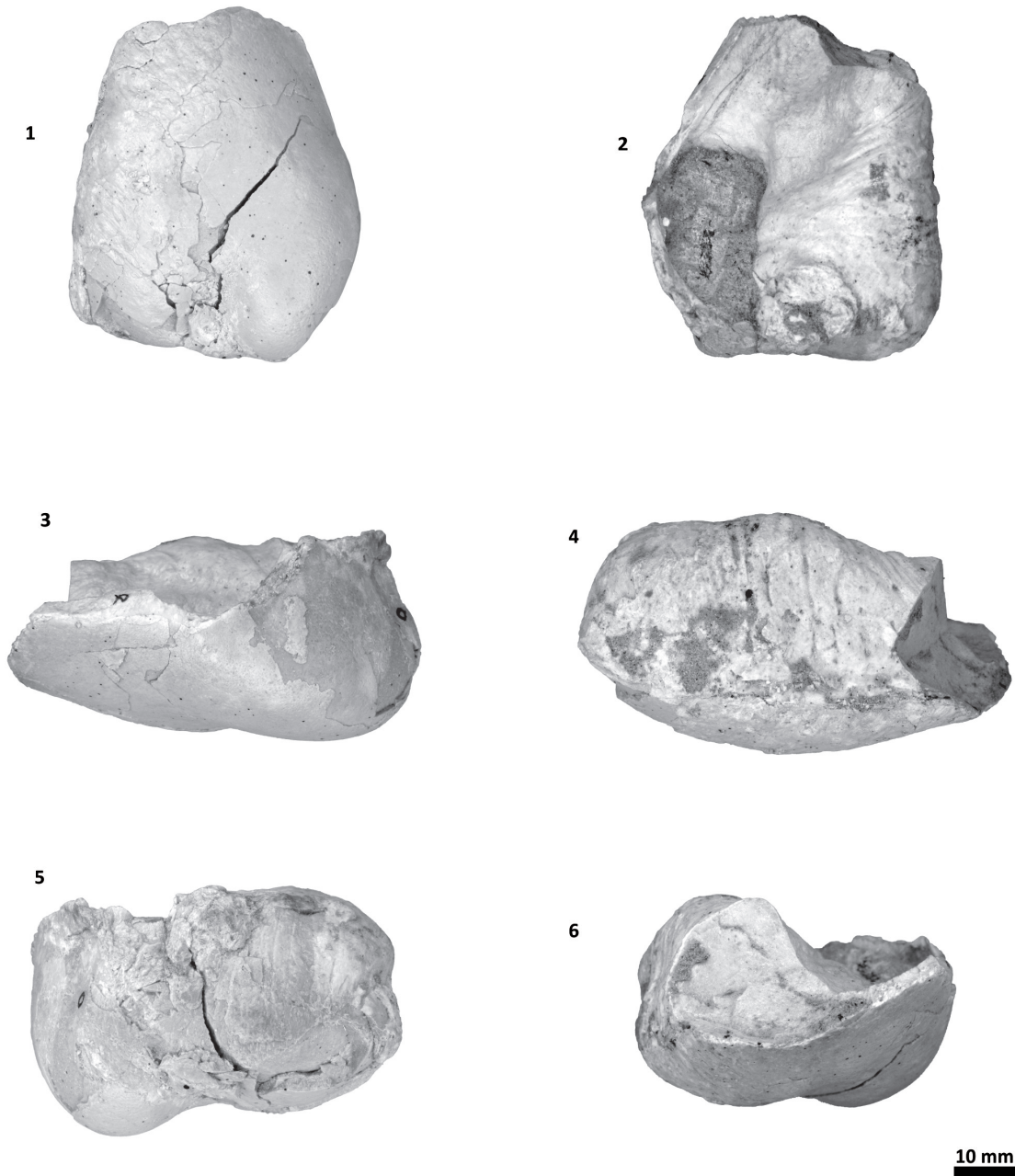


**FIGURE 20.** Left bulla, *Tlaxcallicetus* sp. (MU EcSj5/18/95), ventral (1), dorsal (2), lateral (3), medial (4), posterior (5), and anterior (6) views.

rior or posterior view (120/5); as well as an anterior process of periotic in lateral view, ovoid or antero-posteriorly compressed with a prominent anterodorsal angle in linguiform shape (146/3). These latter characters are autapomorphies for *Tlaxcallicetus* and are unknown in *Sitsqwayk*. Note these autapomorphic characters are not reflected in equal weights results.

In general, the trees' topology is close to that obtained by Marx and Fordyce (2015). Results support poorly *Tlaxcallicetus* as a taxon in both phylogenetic tests. The crown Mysticeti, which "includes all the extant species and all the descendants of the most recent common ancestor of living Mysticeti" (Tsai and Fordyce, 2016), is gathered into the following groups: Balaenidae, Cetotheriidae, and Balaenopteroidea. Stem groups as Llano-

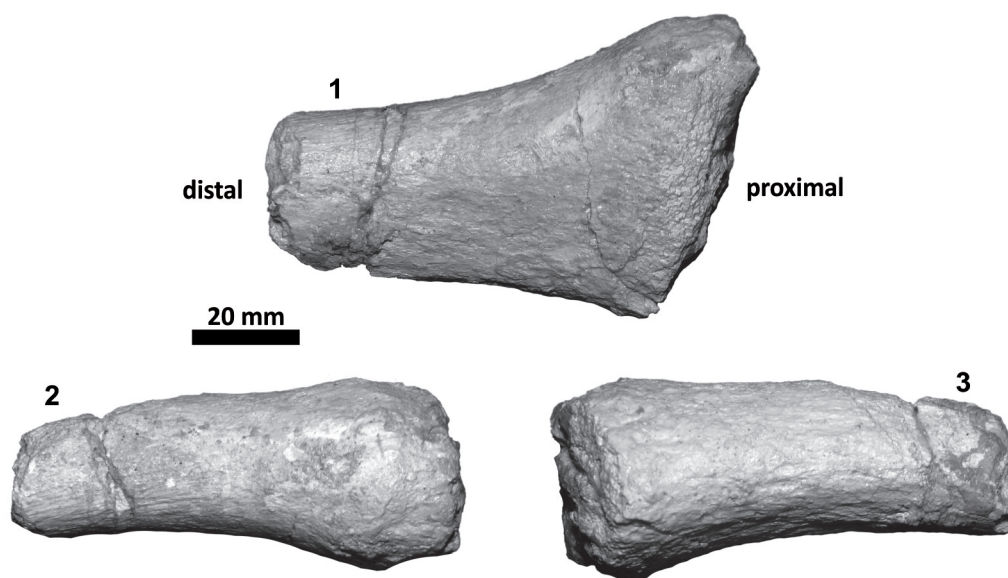


**FIGURE 21.** Left thyrohyoid, *Tlaxcallicetus* sp. (MU EcSj5/18/95), dorsal (1), anterior (2), and posterior (3) views.

cetidae, Mammalodontidae, and Eomysticetidae are equable. *Horopeta* and *Whakakai* conserved its positioning near the crown similar to the analysis of Tsai and Fordyce (2016), *Mauicetus* exhibits an ambiguous position among the stem- and crown Mysticeti, and *Sitsqwayk* is still near to Eomysticetidae (Peredo and Uhen, 2016) but now beside *Tlaxcallicetus*.

## DISCUSSION AND CONCLUSION

Like *Mauicetus*, *Whakakai*, *Horopeta*, and *Sitsqwayk*, *Tlaxcallicetus* is an ancient group of extinct mysticetes from the late Oligocene, ~27 Ma. Data suggest that *Tlaxcallicetus* was contemporaneous with the latter Oligocene mysticetes but limited by regions, as well as sympatric in the Northwest of Mexico with other late Oligocene cetaceans, including aetiocetids, eomysticetids, archaic odontocetes, and kekenodontid-like animals (Barnes, 1998; Hernandez-Cisneros and Tsai, 2016; Hernández-Cisneros et al, 2017). Thus, it can be considered as a part of the multiple relict forms of filter-feeders mysticetes that were common during late Oligocene (Marx and Fordyce, 2015), which derived from different factors such as evolutionary development (Fordyce and de Mui-zon, 2001; Fitzgerald, 2010; Tsai and Fordyce, 2014a, 2014b, 2015b), sympatric speciation events (Clementz et al., 2014), and niche partition (Tsai and Ando, 2015) into heterogeneous environment with varied food sources (Fordyce, 2003; Steeman et al, 2009; Marx and Uhen, 2010). This framework fits the Oligocene mysticetes diversity recorded in

Baja California Sur. Interestingly, *Tlaxcallicetus* belongs to a set of at least ~12 to 14 unnamed distinct morphotypes of early chaeomysticetes recognized for Baja California Sur in the fossil record, which lived in a high productivity, tropical/subtropical environment (Hernandez-Cisneros et al., 2017).

Besides, Oligocene cetacean fossils in Mexico offer a reference point to understand distribution patterns taking into account the feasible influence of Central America Seaway as a migration passage between the Pacific and Atlantic oceans. Furthermore, it is possible that speciation events could have occurred in this geographic space that might connect several early cetacean populations.

On the other hand, *Tlaxcallicetus* contrasts morphologically to the known Oligocene Chaeomysticeti forms, mainly in the periotic bone, which is highly different from others Oligocene mysticetes (see Tsai and Fordyce, 2016). However, absence of morphological data associated to rostrum and mandibles limits interpretation of feeding mechanisms and ecological traits. It is not clear whether *Tlaxcallicetus* was a specialized mysticete by its peculiar morphology, or able to feed as rorquals, via a hypothesized fibrocartilaginous joint between the dentary and the glenoid fossa, indicated by the pitted surface on the fossa's edge (Figure 9). Perhaps the broad paroccipital process present in *Tlaxcallicetus guaycurae* associated to a possible digastric muscle, represents a clue of some feeding behaviour through benthic suction or skimming

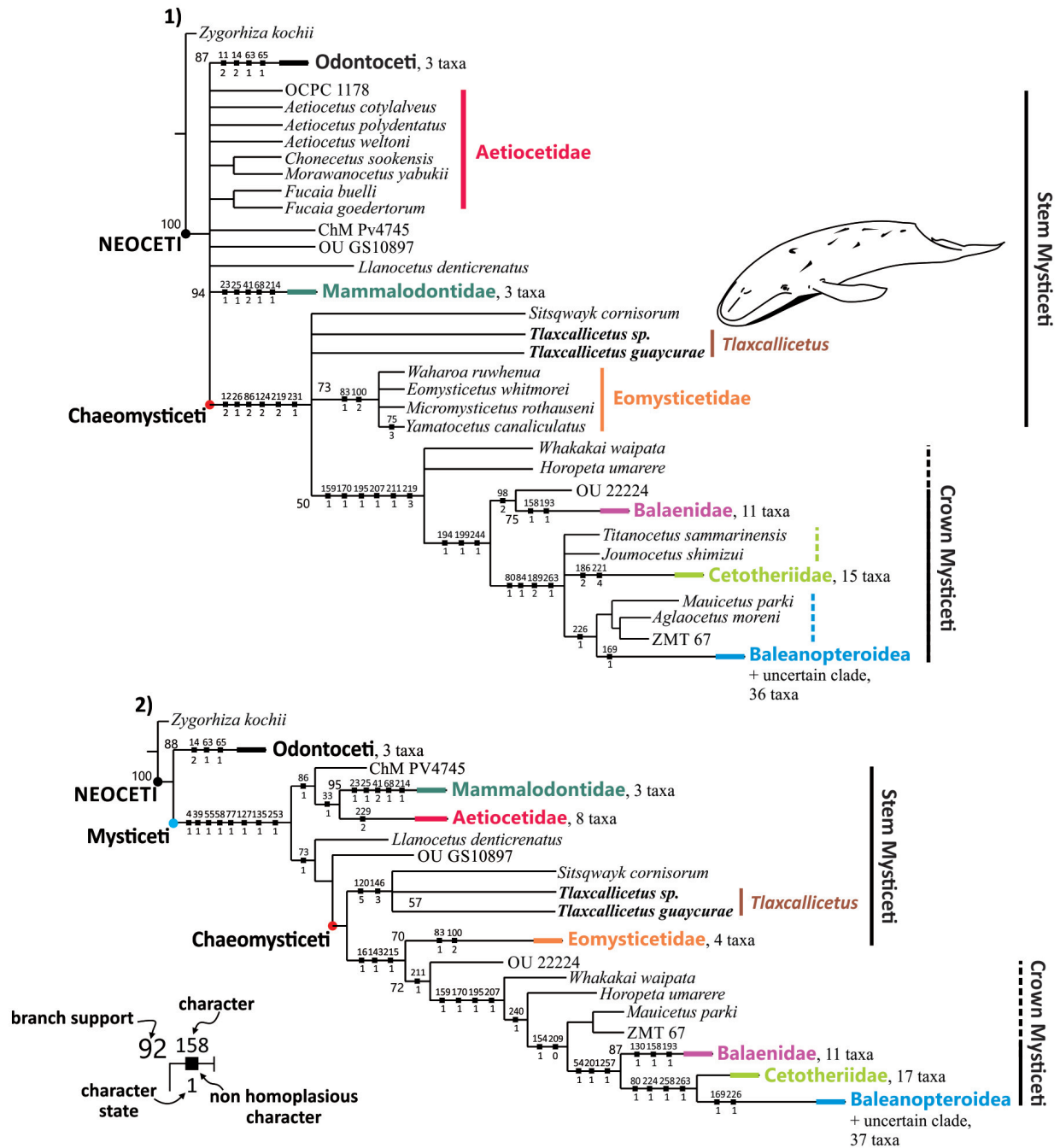


**FIGURE 22.** Phylogenetic position of *Tlaxcallicetus*. 1) Under equal weights, consensus tree recovered from 260 parsimonious trees (1327 steps, consistency index CI= 0.246, retention index RI= 0.686, rescaled consistency index RCI= 0.168756, tree total length 1474). 2) Under implied weights:  $k= 6$ , consensus tree from 3 parsimonious trees (85.63773 steps, CI= 0.271, RI= 0.724, RCI= 0.196204, tree total length 1338). Black squares mark unequivocal characters that support the different groups (see legend). Support branch belongs only to those clades with 50% or more consistency. Dashed lines suggest a probable inclusion of taxa in clade.

(Bouetel, 2005; El Adli and Deméré, 2015), or both. Moreover, the morphological information gap about stem mysticetes as *Tlaxcallicetus* leaves unclear the phylogenetic relations between stem-ward Chaeomyticeti (Tsai and Fordyce, 2015a, 2015b, 2016), as well its phyletic connection through Miocene mysticetes fauna. In conclusion, *Tlaxcallicetus* represents a new form of stem mysticete from the North Pacific Ocean. It is also the first formally described Oligocene mysticete from Mexico, and the southernmost record for this time period in North America.

### ACKNOWLEDGMENTS

I want to thank reviewers J. Velez-Juarbe and C-H. Tsai, as well as the editors, for their assistance and comments. I am also grateful to G. Aguirre-Fernández, Y. Tanaka, J.J. Morrone, and B.L.

Beatty for their comments and constructive criticism during the preparation of this paper. Moreover, to E. H. Nava-Sánchez for his support field work and comments (project SIP: 20131259) as well as T. Schwennicke for his comments on geological details. I'd like to thank G. Gonzalez-Barba for allowing me to take photos and doing this research on the *Tlaxcallicetus* fossils. My appreciation goes to C-H. Tsai for sharing and granting access to his photos of *Horopeta umarere*, as well as to many people who helped in different ways. This study was a result of AEHC's MSc thesis at the Instituto Politécnico Nacional – Centro Interdisciplinario de Ciencias Marinas (CICIMAR-IPN), supported by the Consejo Nacional de Ciencia y Tecnología (CONACYT), scholarship 290143, from 2012 to 2014.

### REFERENCES

- Barnes, L.G. 1998. The sequence of fossil marine mammal assemblages in México, p. 26-79. In Carranza-Castañeda, O. and Córdoba-Méndez, D.A (eds.), *Avances en Investigación, Paleontología de Vertebrados: México*. Universidad Autónoma del Estado de Hidalgo, Pachuca, Hidalgo, México.
- Barnes, L.G., Kimura, M., Furusawa, H., and Sawamura, H. 1995. Classification and distribution of Oligocene Aetiocetidae (Mammalia; Cetacea; Mysticeti) from western North America and Japan. *The Island Arc*, 3:392-431. <https://doi.org/10.1111/j.1440-1738.1994.tb00122.x>
- Benham, W.B. 1937. On *Lophocephalus*, a new genus of zeuglodont Cetacea. *Transactions and Proceedings of the Royal Society of New Zealand*, 67:1-7.
- Berggren, W.A., Kent, D.V., Swisher III, C.C., and Aubry, M-P. 1995. A revised Cenozoic geochronology and chronostratigraphy, p. 129-212. In Berggren, W.A., Kent, D.V., Aubry, M.-P., and Hardenbol, J. (eds.), *Geochronology, Time Scales and Global Stratigraphic Correlation*, Special Publication. Society of Economic Paleontologists and Mineralogists, Tulsa, Oklahoma, USA.
- Boessenecker, R.W. and Fordyce, R.E. 2014. A new eomysticetid (Mammalia: Cetacea) from the late Oligocene of New Zealand and a reevaluation of "*Mauicetus*" *waitakiensis*. *Papers in Palaeontology*, 1:107-140. <https://doi.org/10.1002/spp2.1005>
- Boessenecker, R.W. and Fordyce, R.E. 2015a. A new genus and species of eomysticetid (Cetacea: Mysticeti) and a reinterpretation of '*Mauicetus*' *lophocephalus* Marples, 1956: Transitional baleen whales from the upper Oligocene of New Zealand. *Zoological Journal of the Linnean Society*, 175:607-660. <https://doi.org/10.1111/zoj.12297>
- Boessenecker, R.W. and Fordyce, R.E. 2015b. Anatomy, feeding ecology, and ontogeny of a transitional baleen whale: a new genus and species of Eomysticetidae (Mammalia: Cetacea) from the Oligocene of New Zealand. *PeerJ*, 1-69. 3:e1129; <https://doi.org/10.7717/peerj.1129>
- Bouetel, V. 2005. Phylogenetic implications of skull structure and feeding behavior in balaenopterids (Cetacea, Mysticeti). *Journal of Mammalogy*, 86:139-146.
- Brisson, M.-J. 1762. *Regnum Animale in classes IX distributum, sive synopsis methodical*. Lugduni Batavorum, Netherlands.
- Clementz, M.T., Fordyce, R.E., Peek, S.L., and Fox, D.L. 2014. Ancient marine isoscapes and isotopic evidence of bulk-feeding by Oligocene cetaceans. *Palaeogeography, Palaeoclimatology, Palaeoecology*, 400:28-40. <https://doi.org/10.1016/j.palaeo.2012.09.009>
- Congreve, C.R. and Lamsdell, J.C. 2016. Implied weighting and its utility in palaeontological datasets: a study using modelled phylogenetic matrices. *Palaeontology*, 59:447-462. <https://doi.org/10.1111/pala.12236>

- El Aldi, J.J. and Deméré, T.A. 2015. On the anatomy of the temporomandibular joint and the muscles that act upon it: observations on the gray whale, *Eschrichtius robustus*. *The Anatomical Record*, 298:680-690. <https://doi.org/10.1002/ar.23109>
- Evans, H.D. and de Lahunta, A. 2013. *Miller's Anatomy of the Dog* (fourth edition). Elsevier, China.
- Fischer, R., Galli-Olivera, C., Gidde, A., and Schwennicke, T. 1995. The El Cien Formation of southern Baja California, México: Stratigraphic precisions. *Newsletters on Stratigraphy*, 32:137-161. <https://doi.org/10.1127/nos/32/1995/137>
- Fitzgerald, E.M.G. 2010. The morphology and systematics of *Mammalodon colliveri* (Cetacea: Mysticeti), a thoothed mysticete from the Oligocene of Australia. *Zoological Journal of the Linnean Society*, 158:367-476. <https://doi.org/10.1111/j.1096-3642.2009.00572.x>
- Fordyce, R.E. 1980. Whale evolution and Oligocene southern ocean environments. *Palaeogeography, Palaeoclimatology, Palaeoecology*, 31:319-336. [https://doi.org/10.1016/0031-0182\(80\)90024-3](https://doi.org/10.1016/0031-0182(80)90024-3)
- Fordyce, R.E. 1992. Cetacean evolution and Eocene/Oligocene environments, p. 368-381. In Prothero, D.R. and Berggren, W.A. (eds.), *Eocene-Oligocene Climatic and Biotic Evolution*. Princeton University Press, Princeton, New Jersey, USA.
- Fordyce, R.E. 2003. Cetacean evolution and Eocene-Oligocene oceans revisited, p. 154-170. In Prothero, D.R., Ivany, L.C., and Nesbitt, E.A. (eds.), *From Greenhouse to Icehouse: The Marine Eocene-Oligocene Transition*. Columbia University Press, New York, New York, USA.
- Fordyce, R.E. 2009a. Cetacean evolution. p. 201-207. In Perrin, W.F., Thewissen, J.G.M., and Würsig, B. (eds.), *Encyclopedia of Marine Mammals*. Elsevier, San Diego, CA, USA.
- Fordyce, R.E. 2009b. Neoceti. p. 758-763. In Perrin, W.F., Thewissen, J.G.M., and Würsig, B. (eds.), *Encyclopedia of Marine Mammals*. Elsevier, San Diego, CA, USA.
- Fordyce, R.E. 2009c. Cetacean fossil record. p. 207-215. In Perrin, W.F., Thewissen, J.G.M., and Würsig, B. (eds.), *Encyclopedia of Marine Mammals*. Elsevier, San Diego, CA, USA.
- Fordyce, R.E. 2009d. Fossil sites, Noted. p. 459-466. In Perrin, W.F., Thewissen, J.G.M., and Würsig, B. (eds.), *Encyclopedia of Marine Mammals*. Elsevier, San Diego, CA, USA.
- Fordyce, R.E. and de Muizon, C. 2001. Evolutionary history of whales: a review, p. 169-234. In Mazin, J.-M. and de Buffrenil, V. (eds.), *Secondary Adaptation of Tetrapods to Life in Water*. Pfeil, München, Germany.
- Gatesy J., Geisler, J.H., Chang, J., Buell, C., Berta, A., Meredith, R.W., Springer, M.S., and McGowen, M.R. 2013. A phylogenetic blueprint for a modern whale. *Molecular Phylogenetics and Evolution*, 66:479-509. <https://doi.org/10.1016/j.ympev.2012.10.012>
- Geisler, J.H., Boessenecker, R.W., Brown, M. and Beatty, B.L. 2017. The origin of filter feeding in whales. *Current Biology*, 27:1-7. <https://doi.org/10.1016/j.cub.2017.06.003>
- Geisler, J.H. and Luo, Z. 1996. The petrosal and inner ear of *Herpetocetus* sp. (Mammalia: Cetacea) and their implications for the phylogeny and hearing of archaic mysticetes. *Journal of Paleontology*, 70:1045-1066. <https://doi.org/10.1017/S0022336000038749>
- Geisler, J.H., McGowen, M.R., Yang, G., and Gatesy J. 2011. A supermatrix analysis of genomic, morphological, and paleontological data from crown Cetacea. *BMC Evolutionary Biology*, 11:112. <https://doi.org/10.1186/1471-2148-11-112>
- Goloboff, P.A. 1993. Estimating character weights during tree search. *Cladistics*, 9:83-91. <https://doi.org/10.1006/clad.1993.1003>
- Goloboff, P.A., Farris, J.S., Källersjö M., Oxelman B., Ramírez M.J., and Szumik C.A. 2003. Improvements to resampling measures of group support. *Cladistics*, 19:324-332. <https://doi.org/10.1111/j.1096-0031.2003.tb00376.x>
- Goloboff, P.A., Farris, J.S., and Nixon, K.C. 2008a. TNT, a free program for phylogenetic analysis. *Cladistics*, 24:774-786. <https://doi.org/10.1111/j.1096-0031.2008.00217.x>
- Goloboff, P.A., Carpenter, J.M., Arias, J.S., and Miranda-Esquivel, D.R. 2008b. Weighting against homoplasy improves phylogenetic analysis of morphological data sets. *Cladistics*, 24:1-16. <https://doi.org/10.1111/j.1096-0031.2008.00209.x>
- Gray, J.E. 1864. On the cetaceous mammals, p. 1-53. In Richardson, J. and Gray, J.E. (eds.), *The Zoology of the Voyage of the H.M.S. Erebus and Terror, under the Command of Capt. Sir. JC Ross, RN, FRS, during the Years 1839–1843, Vol. 1 & 2*. E.W. Janson, London, UK.
- Hausback, B.P. 1984. Cenozoic volcanic and tectonic evolution of Baja California Sur, Mexico, p. 219-236. In Frizzell, V.A. (ed.). *Geology of the Baja California Peninsula*, S.E.P.M. Pac. Sect. Los Angeles, CA, USA.

- Hernández-Cisneros, A.E. and Tsai, C-H. 2016. A possible enigmatic kekenodontid (Cetacea, Kekenodontidae) from the Oligocene of Mexico. *Paleontología Mexicana*, 5:147-155.
- Hernández-Cisneros, A.E., González-Barba, G., and Fordyce R.E. 2017. Oligocene cetaceans from Baja California Sur, Mexico. *Boletín de la Sociedad Geológica Mexicana*, 69:149-173.
- Kim, W.H. and Barron, J.A. 1986. Diatom biostratigraphy of the upper Oligocene to lowermost Miocene San Gregorio Formation, Baja California Sur. *Diatom Research*, 1:169-187. <https://doi.org/10.1080/0269249X.1986.9704967>
- Lambertsen, R., Ulrich, N., and Straley, J. 1995. Frontomandibular stay of Balaenopteridae: a mechanism for momentum recapture during feeding. *Journal of Mammalogy*, 76(3):877-899.
- Marx, F.G. and Fordyce, R.E. 2015. Baleen boom and bust: a synthesis of mysticete phylogeny, diversity and disparity. *Royal Society Open Science*, 2:140434. <https://doi.org/10.1098/rsos.140434>
- Marx, F.G. and Uhen, M.D. 2010. Climate, critters, and cetaceans: cenozoic drivers of the evolution of modern whales. *Science*, 327:993-996. <https://doi.org/10.1126/science.1185581>
- Marx, F.G., Tsai, C-H., and Fordyce, R.E. 2015. A new early Oligocene toothed 'baleen' whale (Mysticeti: Aetiocetidae) from western North America: one of the oldest and the smallest. *Royal Society Open Science*, 2:150476. <https://doi.org/10.1098/rsos.150476>
- Mead, J.G. and Fordyce, R.E. 2009. The therian skull: a lexicon with emphasis on the odontocetes. *Smithsonian Contributions to Zoology*, 627:1-248.
- Mitchell, E.D., 1989. A new cetacean from the late Eocene La Meseta Formation, Seymour Island, Antarctic Peninsula. *Canadian Journal of Fisheries and Aquatic Science*, 46:2219-2235. <https://doi.org/10.1139/f89-273>
- Nixon, K.C. 2002. WinClada ver. 1.00.08. Published by the author, Ithaca, New York, USA. <http://www.diversityoflife.org/winclada/>
- Oishi, M. and Hasegawa, Y. 1994. Diversity of Pliocene mysticetes from eastern Japan. *The Island Arc*, 3:436-452. <https://doi.org/10.1111/j.1440-1738.1994.tb00124.x>
- Peredo, C.M. and Uhen, M.D. 2016. A new basal chaeomysticete (Mammalia: Cetacea) from the late Oligocene Pysht Formation of Washington, USA. *Papers in Palaeontology*, 2:533-554. <https://doi.org/10.1002/spp2.1051>
- Plata-Hernández, E. 2002. *Cartografía y estratigrafía del área de Tembabichi, Baja California Sur, México*. Unpublished Bachelors Thesis, Universidad Autónoma de Baja California Sur, Baja California Sur, Mexico.
- Pynson, N.D. and Sponberg, S.N. 2011. Reconstructing body size in extinct crown Cetacea (Neoceti) using allometry, phylogenetic methods and tests from the fossil record. *Journal of Mammalian Evolution*, 18:269-288. <https://doi.org/10.1007/s10914-011-9170-1>
- Sanders, A.E. and Barnes, L.G. 2002a. Paleontology of the late Oligocene Ashley and Chandler Bridge formations of South Carolina, 2: *Micromysticetus rothauseni*, a primitive cetotheriid mysticete (Mammalia: Cetacea). *Smithsonian Contributions to Paleobiology*, 93:271-293.
- Sanders, A.E. and Barnes, L.G. 2002b. Paleontology of the late Oligocene Ashley and Chandler Bridge Formations of South Carolina, 3: Eomysticetidae, a new family of primitive mysticetes (Mammalia: Cetacea). *Smithsonian Contributions to Paleontology*, 93:313-356.
- Schwennicke, T. 1994. Deep and shallow water phosphorite-bearing strata of the Upper Oligocene of Baja California, Mexico (San Juan Member, El Cien Formation). *Zentralblatt Geologie Paläontologie*, 1:567-580.
- Smith, J.T. 1991. Cenozoic marine mollusks and paleogeography of the Gulf of California. p. 637-666. In Dauphin, J.P. and Simoneit, R.T. (eds.), *The Gulf and Peninsular Province of the Californias*, Memoir 47. American Association of Petroleum Geologists, Tulsa, Oklahoma, USA.
- Steeman, M.E. 2010. The extinct baleen whale fauna from the Miocene-Pliocene of Belgium and the diagnostic cetacean ear bones. *Journal of Systematic Palaeontology*, 8:63-80. <https://doi.org/10.1080/14772011003594961>
- Steeman, M.E., Hebsgaard, M.B., Fordyce, R.E., Ho, S.Y.W., Rabosky, D.L., Nielsen, R., Rahbek, C., Glenner, H., Sørensen, M.V., and Willerslev, E. 2009. Radiation of extant cetaceans driven by restructuring of the oceans. *Systematic Biology*, 58:573-585. <https://doi.org/10.1093/sysbio/syp060>
- Swofford, D.L. 1991. PAUP: Phylogenetic Analysis Using Parsimony, Version 3.1. Illinois Natural History Survey, Champaign, Illinois, USA.
- Tsai, C-H. and Fordyce, R.E. 2014a. Disparate heterochronic processes in baleen whale evolution. *Evolutionary Biology*, 41:299. <https://doi.org/10.1007/s11692-014-9269-4>

- Tsai, C-H. and Fordyce, R.E. 2014b. Juvenile morphology in baleen whale phylogeny. *Naturwissenschaften*, 101:765. <https://doi.org/10.1007/s00114-014-1216-9>
- Tsai, C-H. and Fordyce, R.E. 2015a. The earliest gulp-feeding mysticete (Cetacea: Mysticeti) from the Oligocene of New Zealand. *Journal of Mammal Evolution*, 22:355. <https://doi.org/10.1007/s10914-015-9290-0>
- Tsai, C.-H. and Fordyce, R.E. 2015b. Ancestor-descendant relationships in evolution: origin of the extant pygmy right whale, *Caperea marginata*. *Biology Letters* 11(1):20140875. <https://doi.org/10.1098/rsbl.2014.0875>
- Tsai, C-H. and Fordyce R.E. 2016. Archaic baleen whale from the Kokoamu Greensand: earbones distinguish a new late Oligocene mysticete (Cetacea: Mysticeti) from New Zealand. *Journal of the Royal Society of New Zealand*, 46:1-22. <https://doi.org/10.1080/03036758.2016.1156552>
- Tsai, C-H. and Ando, T. 2015. Niche partitioning in Oligocene toothed mysticetes (Mysticeti: Aetiocetidae). *Journal of Mammal Evolution*, 23:33. <https://doi.org/10.1007/s10914-015-9292-y>
- Uhen, M.D. and Pyenson, N.D. 2007. Diversity estimates, biases, and historiographic effects: resolving cetacean diversity in the Tertiary. *Palaeontologia Electronica* 10.2.11A:22p, 754kb; [http://palaeo-electronica.org/2007\\_2/00123/index.html](http://palaeo-electronica.org/2007_2/00123/index.html)
- Walsh, B.M and Berta, A. 2011. Occipital ossification of balaenopteroid mysticetes. *The Anatomical Record*, 294:391-398. <https://doi.org/10.1002/ar.21340>
- Whitmore, F.C. and Sanders, A.E. 1976. Review of the Oligocene Cetacea. *Systematic Zoology*, 25:304-320. <https://doi.org/10.2307/2412507>

#### **APPENDIX 1.**

NEXUS file. All appendices are online at [palaeo-electronica.org/content/2018/2147-oligocene-mysticetes-from-mexico](http://palaeo-electronica.org/content/2018/2147-oligocene-mysticetes-from-mexico).

#### **APPENDIX 2.**

Character map, equal weights analysis. Character map, implied weights analysis (k=6). All appendices are online at [palaeo-electronica.org/content/2018/2147-oligocene-mysticetes-from-mexico](http://palaeo-electronica.org/content/2018/2147-oligocene-mysticetes-from-mexico).

#### **APPENDIX 3.**

Phylogenetic arrangement under implied weights analysis (k=3). All appendices are online at [palaeo-electronica.org/content/2018/2147-oligocene-mysticetes-from-mexico](http://palaeo-electronica.org/content/2018/2147-oligocene-mysticetes-from-mexico).

#### **APPENDIX 4.**

Phylogenetic relation of *Tlaxcallicetus*. Equal weights analysis, strict consensus of 260 equally parsimonious trees. Tree length is 1474. The number in each branch denotes the branch length. All appendices are online at [palaeo-electronica.org/content/2018/2147-oligocene-mysticetes-from-mexico](http://palaeo-electronica.org/content/2018/2147-oligocene-mysticetes-from-mexico).

#### **APPENDIX 5.**

Phylogenetic relation of *Tlaxcallicetus*. Implied weights analysis (k=6), strict consensus of three equally parsimonious trees. Tree length is 1338. The number in each branch denotes the branch length. All appendices are online at [palaeo-electronica.org/content/2018/2147-oligocene-mysticetes-from-mexico](http://palaeo-electronica.org/content/2018/2147-oligocene-mysticetes-from-mexico).

#### **APPENDIX 6.**

Backbone constraint tree data. All appendices are online at [palaeo-electronica.org/content/2018/2147-oligocene-mysticetes-from-mexico](http://palaeo-electronica.org/content/2018/2147-oligocene-mysticetes-from-mexico).